Ecology, not host phylogeny, shapes the oral microbiome in closely related species of gorillas

Markella Moraitou[1#], Adrian Forsythe[1#], James A. Fellows Yates[2,3], Jaelle C. Brealey[4], Christina Warinner[2,3,5,6], Katerina Guschanski[1,7,8, *]

[1]Animal Ecology, Department of Ecology and Genetics, Uppsala University, 75236 Uppsala, Sweden

[2]Department of Archaeogenetics, Max Planck Institute for Evolutionary Anthropology, 04103 Leipzig, Germany

[3]Department of Paleobiotechnology, Leibniz Institute for Natural Product Research and Infection Biology Hans Knöll Institute, 07745 Jena, Germany

[4]Department of Natural History, NTNU University Museum, Norwegian University of Science and Technology, 7491 Trondheim, Norway

[5]Faculty of Biological Sciences, Friedrich Schiller University, 07743 Jena, Germany

[6]Department of Anthropology, Harvard University, Cambridge, MA 02138

[7]Science for Life Laboratory, 75237 Uppsala, Sweden

[8]Institute of Evolutionary Biology, School of Biological Sciences, University of Edinburgh, Edinburgh EH9 3FL, United Kingdom

[#]These authors contributed equally

[*]Correspondence email: katerina.guschanski@ed.ac.uk; markella.mor@gmail.com; adrian.e.forsythe@gmail.com

Key words: ancient DNA, dental calculus, museum specimens, gorilla, metagenome-assembled genomes, shotgun metagenomics

Abstract

Host-associated microbiomes are essential for a multitude of biological processes. Placed at the contact zone between external and internal environments, the little-studied oral microbiome has important roles in host physiology and health. Here we investigate the contribution of host evolutionary relationships and ecology in shaping the oral microbiome in three closely related gorilla subspecies (mountain, Grauer's, and western lowland gorillas) using shotgun metagenomics of 46 museum-preserved dental calculus samples. We find that the oral microbiomes of mountain gorillas are functionally and taxonomically distinct from the other two subspecies, despite close evolutionary relationships and geographic proximity with Grauer's gorillas. Grauer's gorillas show intermediate bacterial taxonomic and functional, and dietary profiles. Altitudinal differences in gorilla subspecies ranges appear to explain these patterns, proposing a close connection between dental calculus microbiome and the environment, which is further supported by the presence of gorilla subspecies-specific phyllosphere/rhizosphere taxa. Mountain gorillas show high abundance of nitrate-reducing oral taxa, which may contribute to high altitude adaptation by modulating blood pressure. Our results suggest that ecology, rather than evolutionary relationships and geographic proximity, primarily shape the oral microbiome in these closely related species.

Background

The microbial communities that are found on and inside multicellular organisms are not only remarkably diverse, but also play a crucial role in a vast set of biological processes, such as energy uptake (Arora and Sharma, 2011; Nieuwdorp et al., 2014), detoxification (Nichols et

49 al., 2019; Turner and Bucking, 2019), immune responses (Nikitakis et al., 2017; West et al.,
50 2015) and even neurochemical and hormonal processes that eventually influence behaviour
51 (Suzuki, 2017; Vuong et al., 2017). The extensively studied gut microbiome is shaped by a
52 multitude of factors, including host phylogenetic relationships, social interactions, and dietary
53 adaptations (Moeller et al., 2016; Nishida and Ochman, 2018; Youngblut et al., 2019). In
54 comparison to the gut microbiome, the oral microbiome has received far less attention. Yet, it
55 is of particular importance, as it connects the external and the internal environments and is
56 located directly at the entry point to the digestive and the respiratory tracts. The oral
57 microbiome plays an important role in oral diseases, such as caries and periodontitis, and has
58 been implicated in systemic disorders including cardiovascular disease (Nakano et al., 2011),
59 atherosclerosis (Teles and Wang, 2011), Alzheimer's disease (Olsen and Singhrao, 2015),
60 several cancers (Flynn et al., 2016; Gao et al., 2016) and preterm births (Cobb et al., 2017).

61 Although studies have linked oral microbiome composition to both dietary habits (Adler et al.,
62 2016; Hyde et al., 2014b; Janiak et al., 2021; Nearing et al., 2020) and host evolutionary
63 relationships (Brealey et al., 2020; Ozga and Ottoni, 2021), it is unclear which of the two
64 predominantly drives the evolution of the oral microbiome and how they interact. Early studies
65 suggested that the oral microbiome is strongly heritable and mostly transferred vertically
66 (Corby et al., 2007; Li et al., 2007), with neonate microbiomes resembling those of their
67 mothers (Dominguez-Bello et al., 2010). Moreover, studies in wild animals have indicated that
68 different species harbour distinct oral microbiota (Brealey et al., 2020; Ozga and Ottoni, 2021).
69 Both observations suggest that host evolutionary relationships have a strong effect on oral
70 microbiome structure. Other studies have highlighted the effect of diet on the oral microbiome
71 (Janiak et al., 2021; Wade, 2013), for instance by uncovering differences between young
72 infants and adults of humans and non-human primates, hence providing a potential link with

73 age-related dietary changes (Cephas et al., 2011). However, distinguishing between host
74 evolutionary and ecological factors as well as their contribution to oral microbiome evolution
75 remains difficult, as most previous studies have focused on rather distantly related host species
76 that occupy distinct ecological niches (Boehlke et al., 2020; Li et al., 2013; Smith et al., 2021;
77 Soares-Castro et al., 2019).

78 In recent years, dental calculus - the calcified form of dental plaque that forms on the teeth of
79 mammals - has emerged as a useful material for the study of oral microbiomes across diverse
80 mammalian species (Brealey et al., 2020; Fellows Yates et al., 2021; Ottoni et al., 2019;
81 Warinner et al., 2014). Since dental plaque undergoes periodic mineralizations, it effectively
82 fossilises on the living host, reducing postmortem contamination from environmental
83 microorganisms (Warinner et al., 2015). It thus preserves a snapshot of oral and respiratory
84 microbial communities (Warinner et al., 2014), dietary components (Adler et al., 2013; Radini
85 et al., 2017; Sawafuji et al., 2020) and host DNA (Mann et al., 2018). Museum collections can
86 be efficiently used for the study of oral microbiomes from wild animals (Brealey et al., 2020;
87 Fellows Yates et al., 2021), minimising the exposure and disturbances associated with sampling
88 from live hosts. Furthermore, the detection of damage patterns, a common verification method
89 for ancient DNA (Briggs et al., 2007), can also be implemented on such historical specimens
90 to distinguish endogenous taxa from modern contaminants (Fellows Yates et al., 2021).
91 Previous research suggests that microbial communities in historical and modern dental calculus
92 are remarkably similar (Velsko et al., 2019), therefore studying museum specimens provides
93 reliable information about present-day microbiomes. The exceptional preservation in the
94 calcified matrix also allows assembly of near complete metagenome-assembled genomes
95 (MAGs) (Brealey et al., 2020).

96 In this study, we use dental calculus to uncover ecological and evolutionary factors that drive
97 oral microbiome evolution in a group of closely related species. We focus on gorillas, which
98 consist of two species, western gorilla (*Gorilla gorilla*) and eastern gorilla (*G. beringei*), each
99 of which is further divided into two subspecies. Our sampling covers three of the four
100 subspecies: western lowland gorilla (*G. g. gorilla*), Grauer's gorilla (*G. b. graueri*) and
101 mountain gorilla (*G. b. beringei*). Eastern and western gorillas diverged approximately 250,000
102 years ago, with evidence for substantial gene flow until more recently (McManus et al., 2015;
103 Xue et al., 2015). Western lowland gorillas are found in western equatorial Africa, primarily at
104 low elevations below 500 m above sea level (masl). Their diet consists mainly of various plant
105 parts and fruits (Rogers et al., 2004). The eastern subspecies - mountain and Grauer's gorillas
106 - occur on the eastern side of the Congo basin. They are estimated to have diverged from each
107 other 10,000 years ago (Roy et al., 2014). Grauer's gorillas occupy the largest altitudinal range
108 of all gorillas, ranging from 500 to 2,900 masl (Plumptre et al., 2016). Mountain gorillas are
109 found at even higher elevations, with most of the range of the Virunga Massif population above
110 2,200 masl and extending to up to 3,800 masl. Consequently, these altitudinal differences lead
111 to different dietary profiles among populations and subspecies (Doran et al., 2002; Ganas et
112 al., 2004; Michel et al., 2022; Rogers et al., 2004; van der Hoek et al., 2021), primarily
113 reflecting availability of fruits that are highly seasonal and become scarce with increasing
114 altitude (Ganas et al., 2004).

115 The presence of ecological and dietary differences in these closely related gorilla subspecies
116 provides an opportunity to evaluate the effects of host evolutionary relationships and ecological
117 factors on oral microbiomes. We used shotgun metagenomic sequencing of dental calculus
118 samples from museum specimens (collected between 1910 and 1986) to taxonomically and
119 functionally characterise the oral microbiota, as well as to assemble bacterial MAGs and

120 identify dietary components from the three gorilla subspecies. Between closely related gorilla
121 subspecies, ecology has a large impact on the taxonomic composition and function capacities
122 of the oral microbiome. Our analyses highlight subspecies-specific differences that can be
123 attributed ecological/dietary differences, and bacterial members of the oral microbiome that
124 may contribute to adaptation to high-altitude lifestyle.

125

126 ## Results

127 **Data pre-processing and confirmation of oral microbial signature**

128 We produced paired-end shotgun sequencing data from the gorilla dental calculus of 26 newly
129 collected samples, and complemented these with an additional 31 dental calculus samples from
130 previously published studies (Brealey et al., 2020; Fellows Yates et al., 2021) (Table S1). Four
131 dental calculus samples were sequenced independently in this study and by Fellows Yates et
132 al. (2021). At a later stage of the analysis, this set of technical duplicates allowed us to assess
133 the effect of the dataset in our taxonomic analysis, but only the sample with the largest number
134 of reads for each sample pair was retained for further analyses.

135 Raw sequencing data consisted of, on average, 15,533,319 reads (mean value) per sample
136 (ranging from 1,032 to 95,367,058; Table S1) and 105,653 reads per negative control (both
137 extraction and library preparation, ranging from 19 to 1,132,867; Table S1). After raw sequence
138 pre-processing (which included removal of poly-G tails, adapter and barcode sequences,
139 merging of forward and reverse reads, and quality filtering), *phiX* and gorilla/human sequences
140 were removed by mapping against respective reference genomes and the resulting unmapped
141 reads were used for taxonomic classification using Kraken2 (Wood et al., 2019) with the

142 standard database, which includes all bacterial, archaeal and viral genomes from NCBI.
143 Samples with low read counts, low proportion of oral taxa, as well as duplicate samples (those
144 processed at two different facilities), were removed (Methods). The final dataset consisted of
145 46 dental calculus samples (13 western lowland gorillas, 17 mountain gorilla, 16 Grauer's
146 gorilla; Figure S1), each containing 561,978-77,307,443 reads (mean: 11,365,074, SD:
147 15,577,988; Table S1). We then applied a multi-step procedure, relying on negative controls
148 and museum environmental samples, to remove contaminant taxa (Methods). The final dataset
149 contained a total of 1007 microbial species (in 430 genera), of which 3.4% (n=34) were
150 members of the core hominid oral microbiome (Fellows Yates et al., 2021) and 4.2% (n=42)
151 members of the Human Oral Microbiome Database (HOMD; (Chen et al., 2010); Table S2).
152 These microbial species accounted for ca. 14% of the total microbial non-normalised
153 abundance.

154 The final dataset also included six genera that have been listed as common contaminants by
155 Salter *et al.* (2014) and Weyrich *et al.* (2019), but contain known oral taxa (Chen et al., 2010;
156 Fellows Yates et al., 2021), including *Streptococcus oralis* and *Staphylococcus saprophyticus.*
157 Species belonging to these genera were retained after confirming, where possible, that they
158 exhibit typical post-mortem DNA damage patterns (Methods).

159

160 **Partial mitochondrial genomes from dental calculus allow host subspecies identification**

161 We recovered host mitochondrial sequences from 44 of 46 samples, which we used to confirm
162 gorilla subspecies identity. On average, 31.2% (0.44 - 94.2%; Table S3) of the reference
163 mitochondrial genome was covered by mapped reads, with notable variation in the proportion

164 of genome covered and coverage depth (0.01 - 77.04%, average: 3.27%) between samples.
165 Sample weight (information available for n=24 samples), sample age (n=36), or dataset (newly
166 generated versus previously published by Fellows Yates et al. (2021)) (n=46) did not have an
167 effect on mtDNA genome completeness (ANOVA, p>0.54), whereas host subspecies identity
168 was marginally significant (ANOVA, F-value=3.12, p=0.054). Mountain gorillas had a larger
169 proportion of the mtDNA genome covered by mapped reads than other gorilla subspecies. The
170 cause of this difference is unknown but could be related to factors affecting the shedding of
171 host DNA into the oral environment, such as differences in dietary abrasiveness, salivary flow,
172 or inflammation.

173 To assist with host taxon assignment, we identified 403 diagnostic sites between western and
174 eastern gorillas and 72 diagnostic sites between the two eastern gorilla subspecies (mountain
175 and Grauer's gorillas) using published gorilla mitochondrial genomes (Methods). In most
176 samples, reads mapped to only a small number of diagnostic sites (Table S3). We accepted
177 molecular taxon assignment for samples with reads mapping to at least six diagnostic sites in
178 six separate reads. For six samples, data was insufficient to distinguish between eastern and
179 western gorilla species and for additional six samples we could not reliably distinguish between
180 mountain and Grauer's gorilla subspecies. In these cases, we accepted the host subspecies
181 identification based on museum records, after consulting collection locality, where possible.
182 All but one sample containing a sufficient number of diagnostic sites were successfully
183 assigned to their reported subspecies. The exception was sample MTM010 (museum accession:
184 631168, Swedish Museum of Natural History - NRM), which was confirmed to be a mountain
185 gorilla, in accordance with the museum records, although it was previously reported as a
186 western lowland gorilla based on preliminary genomic information (Fellows Yates et al., 2021).

Oral microbiome diversity and composition differ by host subspecies

We evaluated the differences in microbial alpha diversity between gorilla subspecies by measuring species richness and community evenness (Figure 1). Host subspecies had only a marginal effect on the normalised microbial richness (ANOVA, p=0.061; Figure 1a) but a significant effect on the transformed community evenness (ANOVA, p<0.001; Figure 1b), with the microbial communities of mountain gorillas showing the lowest evenness.

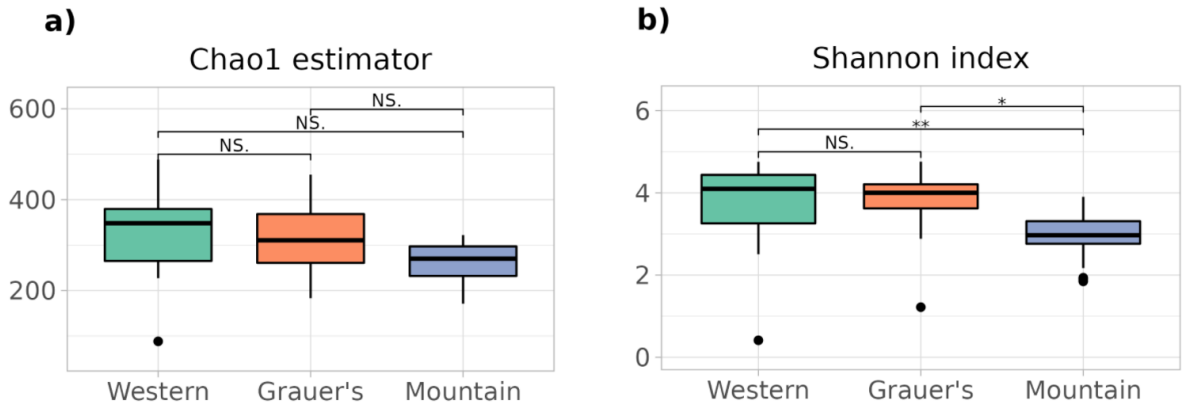

Terms	Mean Squares	F-value	p
Read count	54.37	6.05	**0.018**
Dataset	3.90	0.43	0.513
Subspecies	26.83	2.99	0.061
Residuals	8.98		

Terms	Mean Squares	F-value	p
Read count	4181	6.24	**0.016**
Dataset	887	1.325	0.256
Subspecies	5544	8.28	**0.001**
Residuals	670		

Figure 1. (a) Estimates of community richness, using Chao1 index and (b) community evenness, using Shannon index, alongside corresponding ANOVA results (tables). Pairwise comparisons in (a) and (b) show FDR-adjusted p-values of the Tukey's test (NS=not significant, *p<0.05, **p<0.01). For the ANOVA models, sqrt(500-x) and exp(x) transformations were implemented on the Chao1 estimator and Shannon index values, respectively.

200 Microbiome composition differed by gorilla subspecies (Figure 2, Table 1). This effect
201 persisted even after other potentially confounding factors, such as sequencing depth and
202 dataset, were taken into account. Sequencing depth, included as read count, and dataset were
203 significant factors for the presence-absence-based Jaccard measure, whereas neither of these
204 factors significantly affected relative abundances as estimated with Aitchison distances (Table
205 1). We confirmed that belonging to different datasets had little to no effect on relative
206 abundance by considering three pairs of samples that were derived from the same museum
207 specimen, but were independently sequenced in this study and in Fellows Yates et al. (2021):
208 the duplicate samples appeared close to each other on ordination plots, in particular on the plot
209 based on Aitchison distances (Figure S2). The fourth sample pair (G0004-IBA002) was
210 excluded, as both replicates had lower than 3% oral component, according to microbial source
211 tracking using FEAST (Shenhav et al., 2019) (Figure S3). Pairwise PERMANOVAs
212 (PERMutational ANalysis Of VAriance) (Anderson, 2001) showed strong differentiation
213 between mountain gorillas and the other two subspecies, using both presence-absence and
214 abundance metrics (Table 1). Lastly, we found no significant effect of sex on the oral
215 microbiome using a subset of samples that could be genetically sexed (n=38; Methods; Table
216 S4).

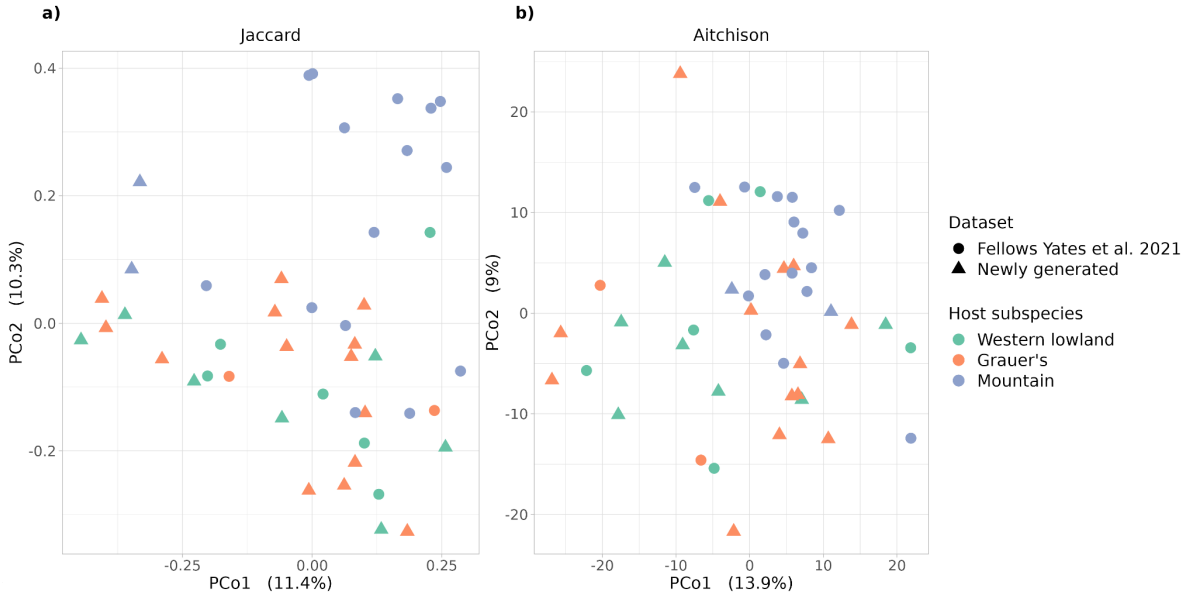

Figure 2. Principal coordinate analysis (PCoA) plots of the individual microbiomes based on a) Jaccard distance and b) Aitchison distance. Host subspecies is displayed in different colours, whereas the dataset is indicated by different shapes (circles for Fellows Yates et al. (2021) and triangles for the newly generated data).

222 **Table 1.** PERMANOVA results, showing the effect size (R^2) and p-value of factors putatively contributing to the
223 variance among sampled microbiota, using Jaccard (reflecting presence-absence of taxa) and Aitchison (reflecting
224 relative abundance of taxa) distances. Pairwise PERMANOVA between subspecies show the effect size (R^2) and
225 p-values adjusted for false discovery rate. P-values below 0.05 are shown in bold.

		Jaccard distances		**Aitchison distances**	
Terms	**Within-factor comparison**	**R^2**	**p**	**R^2**	**p**
Read count		0.069	**< 0.001**	0.023	0.297
Dataset		0.037	**0.005**	0.029	0.083
Subspecies		0.067	**< 0.001**	0.074	**0.001**
	Western lowland vs Grauer's	0.029	0.853	0.041	0.223
	Western Lowland vs Mountain	0.086	**0.001**	0.085	**0.001**
	Grauer's vs Mountain	0.073	**0.001**	0.072	**0.001**
Residuals		0.826	-	0.874	-

226

227 Among the 1007 microbial (species-level) taxa in our dataset, we detected 91 that significantly
228 differed in abundance among gorilla subspecies and 11 that significantly differed in abundance
229 between the datasets, using ANCOM (Mandal et al., 2015) (Table S5). Ten of these 11 taxa
230 also differed in abundance by subspecies but because they could reflect dataset-specific
231 artefacts, we removed the entire genera they belonged to from the list of subspecies-associated
232 taxa. Among the remaining 78 differentially abundant taxa, all but six were absent from at least

233 one host subspecies. The abundances of these taxa were comparable to not differentially
234 abundant taxa (n=929) (t-test: t(123.59)=1.24, p=0.22): 37 taxa ranked above average and 75
235 were in the third quartile of abundance ranks, so that their absence from some host subspecies
236 is unlikely to be explained by non-detection due to low abundance.

237 Mountain gorillas, in particular, appeared to be missing many of these differentially abundant
238 microbial taxa (Figure 3) — which is consistent with the general observation of a marginally
239 reduced microbial richness in this subspecies (Figure 1) — even after accounting for the effect
240 of read depth. Microbial taxa that were absent in mountain gorillas included the orders
241 *Rhodobacteriales*, *Pseudonocardiales*, *Corynebacteriales* (represented mainly by
242 *Corynebacterium* and *Mycolicibacterium*), *Bacillales* (including *Staphylococcus*), and
243 *Rhizobiales* (including bacteria associated with the *Fabaceae* rhizosphere, such as
244 *Agrobacterium deltaense, A. fabacearum* (Delamuta et al., 2020; Yan et al., 2017), and three
245 *Rhizobium* species (Poole et al., 2018)). The presence of rhizosphere- and phyllosphere-
246 associated taxa in the other two subspecies, western lowland and Grauer's gorillas, may reflect
247 habitat or dietary differences among the subspecies. Microbial taxa enriched in mountain
248 gorillas primarily belonged to the orders *Enterobacterales* and certain *Lactobacillales*, like
249 *Streptococcus* sp. and *Lactobacillus gasseri*. The microbiomes of Grauer's gorillas resembled
250 those of western lowland gorillas, both overall (Figure 2, Table 1) and in terms of differentially
251 abundant taxa (Figure 3). However, they also shared some similarities with mountain gorillas
252 (e.g. a presence of *Limosilactobacillus*/*Lactobacillus* species, which were absent in western
253 lowland gorillas), showing an intermediate or mixed composition (Figure 3).

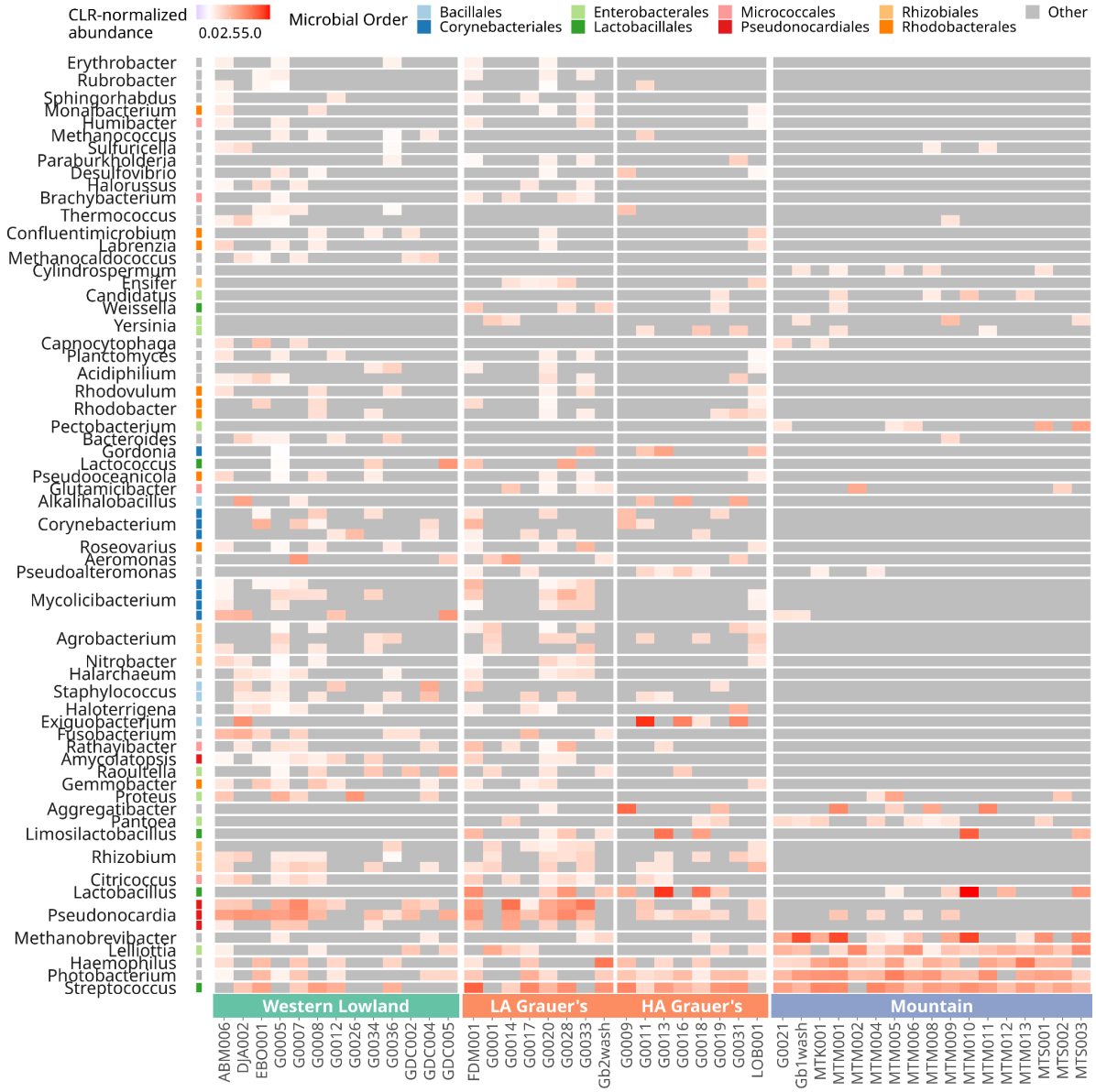

Figure 3. Heatmap depicting centred log-ratio (CLR) normalised abundances of 78 differentially abundant microbial taxa, coloured by taxonomic order (y axis), per sample (x axis). Due to the CLR normalisation, very low abundances or those equal to zero appear as negative values. For clarity, absent taxa (non-normalized abundance equal to zero) are shown in grey.

Gorilla subspecies harbour functionally distinct oral communities

After removing reads mapping to identified contaminants, the retained ("decontaminated") metagenomic reads were functionally characterised with an assembly-free approach using the

263 HUMAnN2 pipeline (Franzosa et al., 2018) (Methods). The normalised abundances of gene
264 families were regrouped under gene ontology (GO) terms, and were aggregated across
265 microbial taxa. Results of functional analyses were broadly consistent with those observed for
266 community-level taxonomy. Specifically, gorilla subspecies was marginally significant
267 (p=0.06) in explaining functional differences in the oral microbiome, whereas neither
268 sequencing depth nor dataset had a significant effect (Table 2). The functional profiles of
269 mountain gorilla microbiomes differed significantly from the other two subspecies (Table 2).

270 We used ANCOM to identify differentially abundant biological processes in the dental calculus
271 microbial communities of the gorilla subspecies, requiring that these processes were
272 represented in at least 30% of the samples in at least one subspecies. Mountain gorillas stood
273 out again, as they missed genes for 236 of the 262 differentially abundant processes (Table S6).
274 In contrast, western lowland and Grauer's gorillas were missing only 13 and 6 processes,
275 respectively. Among six processes that were found in all three gorilla subspecies, mountain
276 gorillas differed significantly from the others in four processes.

277

278 **Table 2**. PERMANOVA results, showing the effect size (R^2) and p-value of factors putatively contributing to the
279 variance in abundance of biological processes among sampled microbiota. Pairwise PERMANOVA between
280 subspecies show the effect size (R^2) and p-values adjusted for false discovery rate. P-values below 0.05 are shown
281 in bold.

Terms	Within-factor comparison	R^2	P
Read count		0.008	0.712
Dataset		0.030	0.220
Subspecies		0.100	0.060
	Western lowland vs Grauer's	0.013	0.695
	Western Lowland vs Mountain	0.124	**0.031**
	Grauer's vs Mountain	0.132	**0.031**
Residuals		0.861	

282

283 **Metagenome-Assembled Genomes**

284 We applied an iterative assembly and binning approach (Methods) to resolve initial MAGs
285 using decontaminated sequencing reads from all samples and museum controls. Across all
286 samples, we constructed a total of eight high-quality (>90% completion, <5% contamination)
287 and 27 medium quality MAGs (>50% completion, <10% contamination), belonging to 24
288 distinct bacterial families (Table S7). Among these 35 MAGs, 25 could be classified to the
289 genus level, with two MAGs assigned to provisional/uncultured genera (UBA8133 and
290 RUG013; Table S7). To place the MAGs within a broader evolutionary context, we constructed

291 a phylogenetic tree including the MAGs and phylogenetically closest bacterial genomes from
292 the Genome Taxonomy Database (GTDB; (Parks et al., 2018); Figure S4). However, for
293 several MAGs assembled in this study we were unable to identify a closely related published
294 genome.

295 Fourteen MAGs reconstructed from dental calculus samples were also present in museum
296 controls (a gorilla skin sample, a gorilla petrous bone, a skull swab and a museum shelf swab).
297 Eight MAGs were present only in the skin sample and only at low abundances (Figure S5).
298 However, five MAGs were found at higher abundance in at least one of the museum controls
299 compared to any gorilla dental calculus sample (Figure S5). This includes MAGs of
300 *Erysipelothrix* (found in gorilla petrous bone), two different *Planococcaceae* (found in the
301 petrous bone and museum shelf swab), as well as *Propionibacterium* and *Exiguobacterium*
302 (both isolated from museum skull swab). These MAGs belong to genera that are common
303 contaminants in metagenomic studies (i.e. *Propionibacterium*, which is a major genus of
304 common skin bacteria (Salter et al., 2014)) and persistent in environmental reservoirs (i.e.
305 *Erysipelothrix*; (Eriksson et al., 2014)). These five MAGs were excluded from downstream
306 analyses. To further authenticate our reconstructed MAGs, we used a collection of isolation
307 source records from public databases of bacterial ecological metadata (Table S8). Taxa with a
308 high proportion (>=25%) of isolation records from sources categorised as
309 environmental/contaminant were considered as potential contaminants (Table S8). Using this
310 approach, we identified 10 additional MAGs that represent likely contaminants (Figures S5&
311 S6).

312 The remaining 20 MAGs recovered here are members of the oral microbiome and are present
313 in databases of common oral taxa (Chen et al., 2010; Fellows Yates et al., 2021). This includes

314 taxa commonly associated with dental plaque communities: *Rothia* (Tsuzukibashi et al., 2017),
315 *Olsenella* (Abusleme et al., 2013; Socransky et al., 1998), *Corynebacterium* (Mark Welch et
316 al., 2016), *Lautropia* (Gerner-Smidt et al., 1994), *Neisseria (Donati et al., 2016)* and
317 *Actinomyces* (Kolenbrander et al., 2010). *Rothia* species are particularly abundant in gorillas
318 compared to humans and other non-human primates (Fellows Yates et al., 2021). Three other
319 MAGs were present in at least 65% of all samples: a MAG most closely related to *Neisseria*
320 (in 95.7% of samples) was found in all Grauer's and mountain gorillas, and the MAGs
321 characterised to the family *Actinomycetaceae* and the genus *Lautropia*, both of which were
322 found in all samples of mountain gorillas (Figure S5).

323 For two MAGs of high completeness and high prevalence in our samples (*Neisseria* and
324 *Limosilactobacillus gorillae*), we produced an alignment of core genes to further investigate
325 how they relate to the known diversity of these taxa. The *Neisseria* MAG clustered with a
326 subset of *Neisseria* species isolated exclusively from humans and was more divergent from
327 *Neisseria* species that formed a clade with isolates from other animals (Figure 4a). Its
328 phylogenetic placement suggests a distinct and not yet identified *Neisseria* taxon. We also
329 recovered a near-complete MAG of *Limosilactobacillus gorillae* (Figure S7), a species
330 previously isolated from faeces of mountain and western lowland gorillas (Tsuchida et al.,
331 2018, 2015). The dental calculus *L. gorillae* MAG was sister to the gorilla faecal isolate but
332 distinct from faecal isolates of other primates (Figure S7a).

333 Oral bacteria play an important role in the metabolism of inorganic nitrate and its reduction to
334 nitrite and nitric oxide, which is essential for the regulation of cardiovascular, metabolic, and
335 neurological processes (Bryan et al., 2017; Hezel and Weitzberg, 2015). Several oral nitrate
336 reducing bacteria, including *Rothia*, *Neisseria*, *Veillonella*, *Corynebacterium*, *Actinomyces*,

337 *Selenomonas*, *Propionibacterium*, *Fusobacterium*, and *Eikenella (Rosier et al., 2022),* were
338 present in gorilla dental calculus samples (Figure S5, Table S5). We used MAGs of *Rothia*,
339 *Neisseria*, and *Veillonella*, which were prevalent in the study samples (Figure S5) to analyse
340 the presence of nitrate-reducing genes in these members of the gorilla oral microbiome.
341 Although we recovered a medium quality MAG of *Corynebacterium* from some samples of
342 western and Grauer's gorillas (Figure S5), it was less prevalent and abundant in gorilla dental
343 calculus and is lacking well-characterised genes involved in nitrate reduction. For *Neisseria*,
344 we could confirm the presence of five nitrate reducates (*nar*), seven genes that provide the
345 cofactor molybdenum to the nitrate reductase enzymes, and four additional genes involved in
346 the regulation of nitrate and nitrite reduction (*aniA*, *nirB*, *nirD*, *norB*; Figure 4a). Only two
347 genes involved in nitrate reduction, *narY* and *mopII*, were not found in the gorilla dental
348 calculus MAG. However, these genes are also absent from other nitrate-reducing oral bacteria
349 (Rosier et al., 2020). Genomic data thus suggests that *Neisseria* isolated from gorilla dental
350 calculus likely has the full capacity to reduce nitrate. The *Neisseria* MAG recovered in this
351 study was significantly more abundant in mountain gorillas compared to the other host
352 subspecies (Figure 4b).

353 *Rothia* and *Veillonella* possessed a smaller repertoire of nitrate-reducing genes compared to
354 *Neisseria*. The *Rothia* MAG recovered in this study had several nitrate reductases and
355 molybdenum cofactor genes, but they differed from genes present in *R. dentocariosa*, a
356 bacterium well studied for its nitrate-reducing capacity (Figure S8; (Rosier et al., 2020). We
357 were also able to identify nine genes involved in nitrate metabolism in *Veillonella*, a well
358 known reducer of nitrate in the oral cavity (Hyde et al., 2014a) (Figure S8). Similar to
359 *Neisseria*, *Veillonella* was significantly more abundant in mountain gorillas than in the other

two gorilla subspecies, whereas the abundance of *Rothia* did not differ among gorilla subspecies (Figure S8b and d).

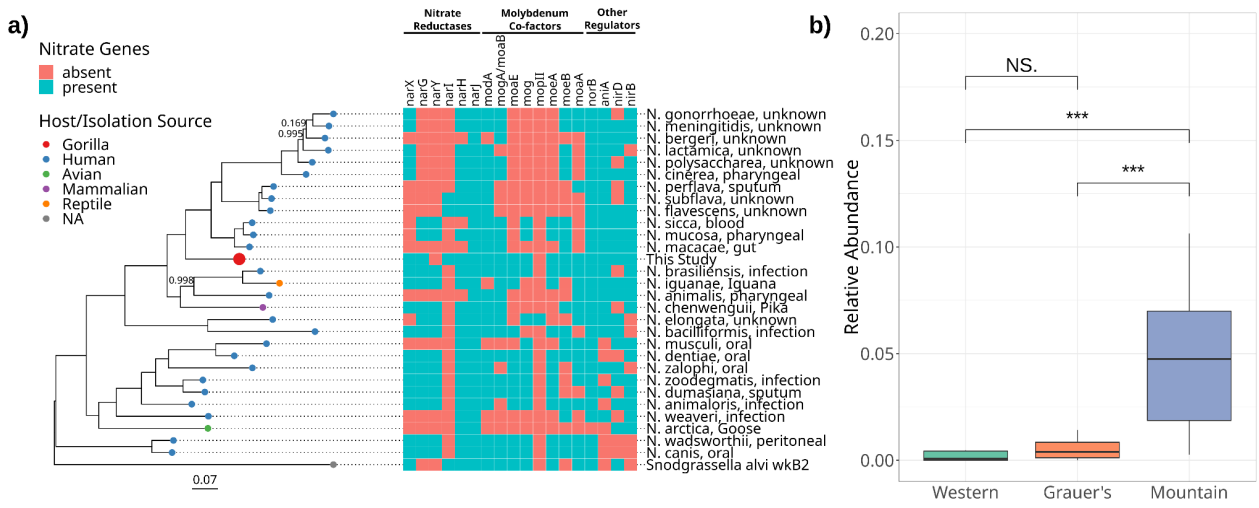

Figure 4: a) Maximum-likelihood phylogeny based on the alignment of core gene sequences from the *Neisseria* MAG and additional published genomes of the same genus. Tip points are coloured by host species identity, and tip labels include the isolation source for each published genome. Scale bar units are the number of substitutions per site and node values represent the proportion of node support out of 100 bootstrap replicates, with unlabeled nodes having complete support (1.0). To the right, the presence of key genes involved in the reduction of nitrate in the oral cavity is shown for each *Neisseria* species. **b)** Relative abundances (CLR transformed) of the *Neisseria* MAG in different gorilla subspecies. The results of a Wilcoxon test are denoted by brackets above boxplots (NS = not significant; *** = p > 0.001).

Altitude may drive oral microbiome composition

Both taxonomic and functional analyses suggest that Grauer's gorilla oral microbiomes are more similar to western lowland gorillas than to mountain gorillas, despite sharing a close evolutionary relationship and an adjacent geographic range with the latter. However, the distribution ranges of all three gorilla subspecies differ in elevation, with mountain gorillas occurring at the highest altitudes. As altitude can influence temperature, humidity and food diversity, which in turn can influence microbial communities, we performed partial Mantel tests between altitudinal distances and taxonomic (Jaccard/Aitchison distances) or functional (Euclidean distance) composition of the oral microbiome, while accounting for log-

381 transformed geographical distance. Geographic location and altitude of the specimens were
382 approximated based on museum records. However, when considering the entire dataset, we did
383 not detect a correlation between altitude and either taxonomy or function (Mantel test: R
384 ranging from -0.13 to 0.06, p>0.12).

385 Since Grauer's gorillas occupy the widest altitudinal range of all gorilla subspecies, we divided
386 Grauer's gorilla samples into high- (>1000 masl, n=8) and low-altitude (≤1000 masl, n=8)
387 groups and tested for differentiation of the oral microbiome both between these groups and
388 among host subspecies. While no compositional differences were identified between the oral
389 microbiomes of western lowland and low altitude Grauer's gorillas using relative abundance
390 measures, western lowland and high altitude Grauer's gorillas displayed marginally significant
391 differences based on pairwise PERMANOVA (FDR-adjusted p-value=0.075, Table 3). The
392 oral microbiome of mountain gorillas consistently differed from other subspecies, independent
393 of altitude grouping (Table 3). Yet, high-altitude Grauer's gorillas showed considerable overlap
394 with mountain gorillas in the first two axes of a PCoA based on Aitchison distances (Figure
395 S9).

396

397 **Table 3.** Results of the pairwise PERMANOVA showing the effect size (R^2) of comparisons of taxonomic
398 composition based on Aitchison distances among four gorilla groups (western lowland, low-latitude Grauer's
399 [≤1000 masl], high-altitude Grauer's [>1000 masl], and mountain gorillas) and the associated p-values (adjusted
400 for false discovery rate). P-values below 0.05 are shown in bold.

Comparison	**R^2**	**p-value (FDR-adjusted)**
Western Lowland vs Low-altitude Grauer's	0.048	0.515
Western Lowland vs High-altitude Grauer's	0.070	0.075
Western Lowland vs Mountain	0.083	**0.002**
Low-altitude Grauer's vs High-altitude Grauer's	0.084	0.164
Low-altitude Grauer's vs Mountain	0.098	**0.002**
High-altitude Grauer's vs Mountain	0.087	**0.002**

401

402 To further investigate the effect of altitude on the oral microbiome, we identified a set of
403 differentially abundant taxa between mountain and western lowland gorillas (n=41) and asked
404 if Grauer's gorillas from different altitudes show similarities with these two subspecies. We
405 observe no significant difference between low-altitude Grauer's and western lowland gorilla
406 and between high-altitude Grauer's and mountain gorillas, whereas all other comparisons were
407 significant ($p<0.003$, Table S9).

408 **Dental calculus reflects dietary differences of gorilla subspecies**

409 After removing reads assigned to bacterial and viral taxa, we performed taxonomic
410 classification of the eukaryotic diversity present within our samples to characterise gorilla
411 dietary components using Kraken2 with the NCBI 'nt' database. Despite applying extensive
412 decontamination procedures (Methods) and removing taxa with few supporting reads (<10),
413 we still recovered erroneous assignments, such as mollusks or other mammals, which gorillas
414 are unlikely to consume (Mann et al., 2020). We therefore restricted our analyses to eukaryotic
415 families that are known to be part of the gorilla diet ((Michel et al., 2022; Remis et al., 2001;
416 Rogers et al., 2004; Rothman et al., 2014; Yamagiwa et al., 2005); Methods). The majority of
417 the 371 genera (65 families) detected in our dataset (Figure S10) were plants (n=360), but we
418 also identified insects, specifically ants, (N=7) and lichen-forming fungi of the *Parmeliaceae*
419 family (N=6).

420 We detected 22 genera that differed in abundance across gorilla subspecies, all belonging to
421 plants, except for the fungal genus *Parmotrema* (Figure 5, Table S10). The broad dietary
422 patterns observed here agree with literature reports. For instance, bamboo - represented here
423 by the African genus *Oldeania*, as well as Asian genera *Phyllostachys*, *Bambusa,* and
424 *Ferrocalamus*, which are likely misclassifications of African bamboo species (Brealey et al.,
425 2020) - was mainly detected in mountain and Grauer's gorillas, as expected (Rothman et al.,
426 2014; Yamagiwa et al., 2005); Figure 5). *Marantochloa* and *Thaumatococcus* of the
427 *Marantaceae* family were detected in western lowland gorillas, which are known to consume
428 them (Rogers et al., 2004), but also in Grauer's gorillas, where the family *Marantaceae* has
429 been reported as part of the diet (Michel et al., 2022). The family Fabaceae is consumed by all
430 gorilla subspecies and the genus *Tamarindus* detected here is likely a misidentification of

431 another member of this family, as *Tamarindus* itself has not been reported to be part of gorilla
432 diet. Grauer's gorillas appear to have the most diverse diet of the three subspecies, consuming
433 foodstuffs typical of both western lowland and mountain gorillas (Figure 5). This is in
434 accordance with the literature (Michel et al., 2022; Remis et al., 2001; Rogers et al., 2004;
435 Rothman et al., 2014; Yamagiwa et al., 2005), which reports 61 plant families as being part of
436 their diet, as opposed to 41 and 45 families for western lowland and mountain gorillas,
437 respectively.

438 Similar to our analyses of differentially abundant bacteria, dietary components which were
439 differentially abundant between mountain and western lowland gorillas showed no significant
440 difference between low-altitude Grauer's and western lowland gorilla and between high-
441 altitude Grauer's and mountain gorillas, while significantly differentiating low- and high-
442 altitude Grauer's gorillas (Table S9).

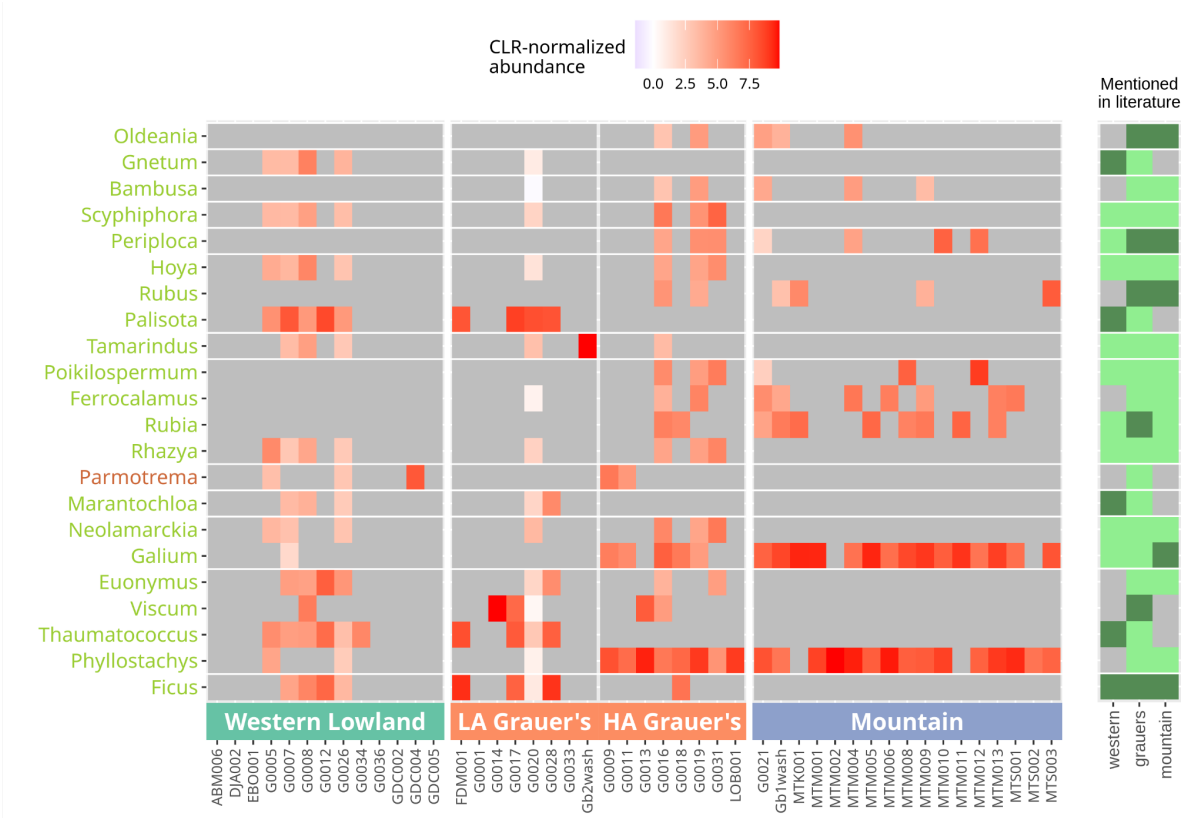

Figure 5. Heatmap based on normalised abundances for differentially abundant dietary taxa at the genus level. For clarity, taxa with abundance equal to 0 are shown in grey. The bars on the right indicate if the family (light green) or the specific genus (dark green) have been reported as part of the diet of each gorilla subspecies (grey: no mention). Horizontal white lines separate plant families.

Discussion

Using three gorilla subspecies, we investigated how evolutionary relationships and ecological factors shape the dental calculus oral microbiome in closely related host taxa. Ecologically, all three subspecies differ from each other, but Grauer's and mountain gorillas are geographically proximate and more closely related to each other than to western lowland gorillas. One of the strongest differences between the three subspecies is the altitude of their ranges, which in turn influences diet, reflected, e.g., in the level of frugivory. Western lowland gorillas occupy the

456 lowest altitudes and are the most frugivorous (Rogers et al., 2004; Takenoshita and Yamagiwa,
457 2008). Mountain gorillas occupy the highest altitude and are the least frugivorous (Ganas et
458 al., 2004; Maisels et al., 2018; Plumptre et al., 2016), whereas Grauer's gorillas live across the
459 largest altitudinal range and hence straddle the ecological conditions faced by both western
460 lowland and mountain gorillas (Yamagiwa et al., 2008). Ecological conditions and dietary
461 differences are expected to affect the host-associated microbial communities (Janiak et al.,
462 2021; Kartzinel et al., 2019; Li et al., 2013; Wade, 2013; Youngblut et al., 2019).

463 By investigating the oral microbiome preserved in dental calculus, we show that oral microbial
464 communities among closely related gorilla subspecies differ, both taxonomically and
465 functionally. In particular, multiple lines of evidence show that the oral microbiome of
466 mountain gorillas differs from the other gorilla subspecies in taxonomic composition, relative
467 abundance, and functional profiles of microbial taxa (Tables 1 and 2), despite the close
468 evolutionary relationship and geographic proximity between mountain and Grauer's gorillas.
469 The oral microbiome of Grauer's gorillas shows strong similarity to western lowland gorillas,
470 although the two species are more distantly related and separated by the Congo Basin. When
471 considering differentially abundant microbial taxa and dietary profiles, Grauer's gorillas
472 appear intermediate, displaying a combination of taxa found in both western lowland and
473 mountain gorillas (Figure 3 and 6). This suggests that host phylogenetic relationships are less
474 important for the structure of the oral microbiome in closely related species than ecological
475 conditions, possibly including diet.

476 These observations deviate from previous studies that identified a phylogenetic signal in the
477 oral microbiome in wild animals. However, these studies compared distantly related species
478 like chimpanzees, humans (Li et al., 2013), other great apes (Boehlke et al., 2020), and even

479 more diverse groups of mammals (Brealey et al., 2020; Ozga and Ottoni, 2021). Often the
480 effects of host phylogenetic relationships and ecology could not be decoupled. For instance,
481 Smith et al. (2021) found differences among three snake species that each occupied a distinct
482 ecological niche. Similarly, Soares-Castro et al. (2019) studied three marine mammals, among
483 which the most evolutionary divergent species also lived in a different habitat, so the effects of
484 ecology were indistinguishable from those of evolutionary relationships.

485 Yet, ecological effects on a short evolutionary scale, as observed in this study, do not preclude
486 co-diversification of the host and its associated microbiome over longer evolutionary time.
487 They rather point to the presence of rapid and dynamic responses of the host-associated
488 microbial communities to environmental conditions, potentially through the seeding of the
489 dental calculus oral microbiome at least to some extent with environmental taxa (see below).
490 In addition, our results are in accordance with other studies that propose external factors, such
491 as diet, influencing the oral microbiome (Adler et al., 2016; Hyde et al., 2014b; Janiak et al.,
492 2021), including Li et al. (2013) who observed that the oral microbiome of captive apes is
493 distinct from their wild counterparts and more similar to other captive apes, highlighting the
494 importance of environmental factors/diet.

495

496 **Oral microbiome diversity might reflect ecology or diet**

497 Our analyses provide a tentative suggestion that ecological differences, approximated here by
498 altitude, may be the primary factor shaping oral microbiome diversity. Specifically, grouping
499 Grauer's gorillas into low- and high-altitude populations, we showed that low-altitude
500 populations harbour an oral microbiome that is indistinguishable from western lowland

501 gorillas, whereas high-altitude populations show near-significant differences (Table 3).
502 Although the oral microbiome of Grauer's gorillas is significantly different from mountain
503 gorillas independent of the altitude, this may be because most mountain gorillas in our dataset
504 were collected above 3000m, notably higher than any of the Grauer's gorilla samples (600-
505 2100m; Table S1). We also observe compositional differences between high- and low- altitude
506 groups of Grauer's gorillas when considering oral and dietary taxa that differentiate mountain
507 and western lowland gorillas (Table S9). The high-altitude populations of Grauer's gorillas
508 appear indistinguishable from mountain gorillas, whereas low-altitude Grauer's gorillas show
509 no differences to western lowland gorillas, supporting the effect of ecological differences
510 connected to altitude that shape microbial and dietary composition. Generally, the dietary
511 profiles of Grauer's gorillas appear to contain dietary items present in both western lowland
512 and mountain gorillas (Figures 6 and S10). Our observation from dental calculus is in line with
513 previous studies (Table S11), which report considerable overlap in the diet of Grauer's gorillas
514 with western lowland (30 of the 41 plant families) and mountain (30 of the 45 plant families)
515 gorillas. In contrast, only 16 dietary families are consumed by both western lowland and
516 mountain gorillas.

517 It is also intriguing to speculate that the local environment itself could affect the composition
518 of the dental calculus community by serving as a source of at least some colonising taxa, for
519 example via the consumed phyllosphere and rhizosphere. A recent study of the human oral
520 microbiome found that specific taxa within the dental plaque community are evolutionarily
521 close to environmental bacteria, whereas those living on the tongue surface are more closely
522 related to other host-associated taxa (Shaiber et al., 2020). This finding suggested that dental
523 plaque microbial communities could be more affected by the environment than other host-
524 associated microbiomes. Within the gorilla oral microbiome, we detected microbial taxa that

525 likely have a dietary origin and differ in abundance among host subspecies, possibly reflecting
526 dietary differences. In particular, bacteria associated with the *Fabaceae* rhizosphere, including
527 *Agrobacterium deltaense, A. fabacearum* (Delamuta et al., 2020; Yan et al., 2017), and three
528 *Rhizobium* species (Poole et al., 2018) may be derived from the consumed dietary items or
529 accidentally ingested soil. These bacteria were significantly more abundant in the dental
530 calculus of western lowland and Grauer's gorillas than in mountain gorillas (Figure 3, Table
531 S5). Two lines of evidence provide a link between these microbial taxa and dietary differences
532 among the gorilla subspecies. First, our data suggest a higher abundance of the family
533 *Fabaceae* in western lowland and Grauer's gorillas (Figures 6 and S10, Table S10) compared
534 to mountain gorillas. Second, although no comparative data exists on the prevalence of roots
535 and rhizomes in the diet of different gorilla species, indirect evidence suggests that western
536 lowland gorillas consume more roots than mountain gorillas. Behavioural observations report
537 frequent root and rhizome consumption in western lowland gorillas of all ages (Fletcher and
538 Nowell, 2008) and comparative dentition analyses show increased tooth wear in western
539 lowland gorillas compared to mountain gorillas, in which tooth wear is well explained by the
540 time spent feeding on roots (Galbany et al., 2016).

541 Although dental calculus is a highly suitable material for the study of the oral microbiome,
542 several previous studies have identified caveats associated with dietary analyses from this
543 source material (Haas et al., 2022; Mann et al., 2020; Ottoni et al., 2019). Sample
544 contamination, the low proportion of eukaryotic reads, and the sparsity of eukaryotic reference
545 databases lead to biases and present a considerable challenge to the analysis of dental calculus.
546 In addition, reference genome contamination can result in false positive taxonomic assignments
547 (Mann et al., 2020). In the present study, the authenticity of putatively dietary taxa could not
548 be assessed using damage patterns due to low abundance of eukaryotic reads. Nevertheless, we

549 were able to detect dietary differences among gorilla subspecies, which are mostly in
550 agreement with previous knowledge of gorilla diets (Figure 5) (Michel et al., 2022; Remis et
551 al., 2001; Rogers et al., 2004; Rothman et al., 2014; Yamagiwa et al., 2005).

552

553 **Metagenome-assembled genomes add to the understanding of wild microbiomes**

554 The recovery of high quality MAGs from metagenomic data can provide an important
555 perspective on the evolutionary relationships among microbial taxa and between
556 microorganisms and their hosts. As reference databases are often biased towards organisms of
557 medical, agricultural, and industrial importance (Marcelino et al., 2020; Velsko et al., 2018),
558 MAGs recovered from novel environments, such as dental calculus oral microbiome of non-
559 human animals, may represent poorly described, understudied or completely unknown
560 microbial lineages (Jiao et al., 2021). Several of the high and medium quality MAGs
561 constructed in this study were recovered in higher abundance from environmental controls than
562 from any dental calculus samples and were considered to represent environmental
563 contaminants. However, other MAGs were highly abundant in the dental calculus samples and
564 belong to taxa that are members of the oral microbiome (Figures S5 & S6). Many of these
565 MAGs were distinct from the evolutionary closest sequenced genomes available in GTDB
566 (Figures S4, S7, S8, Figure 4), suggesting that they may represent undescribed bacterial
567 lineages, in line with discoveries of novel microbial diversity in unstudied host species (Levin
568 et al., 2021; Youngblut et al., 2020). The closest evolutionary relatives of several bacterial taxa
569 with high quality MAGs were found among isolates from primates, including humans (Figures
570 5a, S7, S8).

571 In this study, we recovered a near-complete MAG of *Limosilactobacillus gorillae*, which was
572 more closely related to a faecal isolate from a captive gorilla than to a faecal isolate from
573 another primate (Figure S7a). Usually associated with gorilla faeces (Tsuchida et al., 2014),
574 the presence of *L. gorillae* within the oral microbiome may be the result of coprophagy, a
575 common behaviour among wild gorillas (Graczyk and Cranfield, 2003). However, questions
576 remain regarding the persistence of faecal-associated bacteria within dental calculus and their
577 potential function within the plaque biofilm. Coprophagic behaviour is suggested to serve as a
578 route for vertical or horizontal transmission of gastrointestinal microbiota between individuals
579 (Abusleme et al., 2020) and may have a stabilising impact on host-associated microbial
580 communities overall (Bo et al., 2020).

581 We also reconstructed MAGs of *Neisseria*, *Rothia*, and *Veillonella* and confirmed the presence
582 of nitrate-reducing genes in these members of the gorilla oral microbiome (Figures 5a, S8).
583 The reduction of nitrate to nitrite from dietary sources by oral bacteria provides the precursor
584 to nitric oxide (NO), which is an important signalling and effector molecule (Jones et al., 2021).
585 Along with multiple benefits to circulatory health (Lundberg et al., 2018), nitric oxide is
586 increased in response to hypoxic stress (Feelisch, 2018; Levett et al., 2011), and results in
587 increased blood oxygen levels in the host (Beall et al., 2012). Human populations adapted to
588 high altitude exhale higher concentrations of nitric oxide compared to low-land populations
589 (Beall et al., 2001; Erzurum et al., 2007). For these reasons, regulation of nitric oxide
590 metabolism is thought to be beneficial to high-altitude adaptation (Beall et al., 2012).

591 Mountain gorillas live at elevation of up to 3,800 masl (Williamson et al., 2013) and hence are
592 exposed to hypoxic stress (Ruff et al., 2022). They also show higher abundance of *Neisseria*
593 and *Veillonella* compared to the other two gorilla subspecies, which live at considerably lower

594 altitudes (Figures 5b and S8d). Although it is not known if dietary nitrate amounts differ among
595 gorilla subspecies, the primarily herbivorous diet of mountain gorillas is naturally rich in
596 nitrate. Taken together, it is likely that high abundance of nitrate-reducing oral taxa may aid
597 mountain gorillas cope with the physiological demands of their high-altitude habitat. This
598 finding is particularly intriguing, as comparative genomic analyses failed to uncover host-
599 encoded genes related to high-altitude adaptation in mountain gorillas (Xue et al., 2015). Our
600 results suggest an important role for host-associated microbiomes in promoting host
601 adaptations.

602

603 **Mitochondrial DNA in dental calculus can aid taxonomic assignments of the host**

604 The mitochondrial sequences recovered from the dental calculus metagenomes were used to
605 confirm gorilla subspecies identity. Six of the samples yielded mitochondrial genomes with
606 completeness >80% and coverage >3X (maximum 94% completeness and 77X coverage, Table
607 S3). However, in many cases even a few mitochondrial fragments were sufficient to allow
608 subspecies assignment. We could genetically distinguish gorilla species (eastern versus
609 western gorillas) with mitochondrial genome coverage as low as 2.6% and eastern gorilla
610 subspecies (mountain versus Grauer's) with coverage as low as 6.6%. Grauer's and mountain
611 gorilla mitochondrial genomes could be successfully distinguished despite differing by only
612 0.5% (72 positions, excluding the hypervariable D-loop region (van der Valk et al., 2018)).
613 This observation supports the usefulness of dental calculus as material for obtaining genetic
614 information about the host (Mann et al., 2018; Ozga et al., 2016; Warinner, 2016; Warinner et
615 al., 2015).

616

617 ## Conclusions

618 Our study is, to our knowledge, the first to investigate the evolution of the dental calculus oral
619 microbiome at the early stages of the speciation process of the host and adds to the new but
620 growing field of research on the microbiomes of wild animals. We find that in closely related
621 species, evolutionary relationships are less important than ecology in explaining taxonomic
622 composition and function of the oral microbiome. Host-associated microbial communities have
623 been proposed to contribute to host adaptation, partly because they can respond rapidly to
624 changing environmental conditions (Alberdi et al., 2016). We find that taxa enriched in the
625 mountain gorilla oral microbiome may facilitate their high-altitude lifestyle through increased
626 nitrate reduction potential and the associated physiological benefits. Our discovery of distinct
627 phylo- and rhizosphere taxa in the dental calculus of different gorilla subspecies suggests a
628 close connection between this host-associated microbiome and the local environment.
629 Colonisation of the host by environmental taxa with beneficial functions in local adaptation
630 and health may present an exciting evolutionary route to be explored in the future.

631

632 ## Methods

633 **Sample collection**

634 The study dataset consisted of dental calculus samples from 57 specimens of three gorilla
635 subspecies: 16 western lowlands gorillas, 22 Grauer's gorillas, and 19 mountain gorillas (Table
636 S1). Dental calculus samples of western lowland gorillas were collected at the Royal Museum

637 for Central Africa (RMCA, Tervuren, Belgium) and the Cleveland Museum of Natural History
638 (CMNH, USA). Samples of mountain gorillas came from the Swedish Museum of Natural
639 History (Naturhistoriska Riksmuseet - NRM, Stockholm, Sweden) and the RMCA. Samples of
640 Grauer's gorillas were collected primarily at RMCA, with a few samples from NRM and the
641 Royal Belgian Institute of Natural Sciences (RBINS, Brussels, Belgium). Our dataset consisted
642 of newly generated shotgun data from 26 specimens and published gorilla dental calculus
643 sequences: two samples from Brealey et al. (2020) and 29 samples from Fellows Yates et al.
644 (2021). We also included sequences from 35 published and newly generated extraction blanks,
645 twelve library preparation blanks, and four museum controls. One extraction and one library
646 blank had too few reads for taxonomic classification and were therefore excluded from
647 downstream analysis (Table S1). The museum controls consisted of two swabs taken at NRM
648 from a museum shelf surface holding reindeer (*Rangifer tarandus*) specimens and from the
649 surface of a brown bear (*Ursus arctos*) skull. In addition, we included data from two gorilla
650 specimens from previous studies (van der Valk et al., 2019, 2017): A petrous bone sample from
651 a specimen at NRM and a skin sample from RMCA (ENA accession numbers: ERR2503700
652 and ERR2868193, respectively). These sequences were generated to study the gorilla host,
653 however, we removed host reads and retained microbial reads for our analyses.

654 **Preparation of Genomic Libraries and Metagenomic Shotgun Sequencing**

655 All samples were processed in cleanroom facilities following appropriate methods for working
656 with ancient and historical DNA. DNA was extracted according to the protocol by Dabney et
657 al. (2013) with slight changes, as described in Brealey et al. (2020) and Fellows Yates et al.
658 (2021). The datasets differed in library preparation protocol, indexing strategy, sequencing
659 platform, read length, and sequencing depth (Table S1). Samples from four specimens were

660 processed in both laboratory facilities: Uppsala University, Uppsala, Sweden and the Max
661 Planck Institute for the Science of Human History, Jena, Germany (Fellows Yates et al., 2021).
662 We used these technical duplicates to assess putative batch effects (Fig. S3), but only retained
663 one sample per pair for biological analyses, selecting the one with the largest number of reads.

664 For the newly generated data, we followed the protocol as detailed in Brealey et al. (2021).
665 Briefly, dental calculus samples ranging in weight from < 5 mg and up to 20 mg were surface-
666 decontaminated using UV light (10 min at 254 nm) and washing in 500 µl of 0.5M
667 ethylenediaminetetraacetate (EDTA) for 1 min (Brealey et al., 2021, 2020; Ozga et al., 2016).
668 DNA was extracted using a silica-based method (Dabney et al., 2013) in batches of at most 16
669 samples with two negative controls. DNA was eluted in 45 µl of EB buffer (10 mM tris-
670 hydrochloride, pH 8.0; QIAGEN, Netherlands) supplemented with 0.05% (v/v) Tween-20.

671 Double-stranded genomic libraries for all newly generated and previously sequenced samples
672 were prepared following the double indexing protocol (Dabney and Meyer, 2012; Meyer and
673 Kircher, 2010). Newly generated libraries and those previously published by (Brealey et al.,
674 2020) included double in-line barcodes to guard against index hopping (van der Valk et al.,
675 2020). A detailed protocol for library preparation is provided in Brealey et al. (2020). Library
676 blanks were included for each batch of approximately 20 samples. Adapter-ligated libraries
677 were quantified by a quantitative PCR assay, allowing us to estimate an appropriate number
678 of index PCR cycles, which ranged from 8 to 20. Following indexing, individual libraries were
679 purified with Qiagen MinElute columns and quantified using a quantitative PCR assay. All
680 extraction and library blanks consistently showed lower DNA content than calculus samples
681 (Table S1). We pooled 1.5 µl of each indexed library (including blanks and museum controls)
682 and performed size selection with AMPure XP beads (Beckman Coulter, IN, USA) for

683 fragments of approximately 100-500 bp in length. The pooled library was sequenced by
684 SciLifeLab Uppsala on two Illumina NovaSeq S2 flowcells using paired-end 100 bp read
685 length and V1 sequencing chemistry.

686 **Preprocessing of sequencing data**

687 For each sample, the data generated from different sequencing runs was concatenated into a
688 single file (separately for reverse and forward reads) and poly-G tails, which are artefacts of
689 the two-colour sequencing chemistry of the NextSeq and NovaSeq Illumina platforms, were
690 removed using fastp (V0.20.0; Chen et al., 2018). We removed unpaired reads with BBTools
691 `repair.sh` (V38.61b; Bushnell, 2014). For newly generated data, we used AdapterRemoval
692 (V2.2.2; Schubert et al., 2016) to clip adapters, trim reads based on minimum phred quality
693 (>=30) and length (30bp), and merge forward and reverse reads. The unmerged reads were
694 excluded from downstream analysis (Table S1). In-line barcodes in newly generated data were
695 trimmed from both ends using a Python script (Brealey et al., 2020). Read quality filtering was
696 performed using PrinSeq-Lite (V0.20.4; Schmieder and Edwards, 2011) with a mean base
697 quality threshold of 30. PCR duplicates were removed using a Python script (Brealey et al.,
698 2020), which randomly kept one read among those with the same sequence. All commands and
699 scripts used in our bioinformatic analysis are available at 10.5281/zenodo.6861585.

700 Sequences of the *phi*X bacteriophage, which is used as an internal control for Illumina
701 sequencing (Mukherjee et al., 2015), were removed from the dataset by mapping against the
702 *phiX* genome (GenBank: GCA_000819615.1) using BWA-MEM (V0.7.17; Li and Durbin,
703 2009). Unmapped reads were retained using SAMtools (V1.12; Danecek et al., 2021) and
704 converted to FASTQ for downstream analysis, using the 'bamtofastq' function of BEDtools
705 (V2.29.2; Quinlan and Hall, 2010). To remove host reads and potential human contamination,

706 we mapped all the reads to a combined file containing western lowland gorilla and human
707 reference genomes (GenBank: GCF_000151905.2 and GCF_000001405.38, respectively),
708 repeating the steps above. Extraction blanks, library blanks, and museum controls were only
709 mapped to the human genome. The unmapped reads were used in oral microbiome and dietary
710 analyses, whereas the mapped reads were extracted, sorted, and indexed using SAMtools, and
711 used for the host genomic analyses.

712 **Host genome analysis**

713 *Mitochondrial genome analysis.* From the host mapped BAM files, we extracted all reads
714 mapping to the gorilla mitochondrial genome from position 1 to position 15,446, with a
715 mapping quality of 30 or higher, using SAMtools. Nucleotide positions 15,447-16,364, which
716 contain the D-loop, were excluded to prevent the hypervariable regions from introducing biases
717 in our analyses. We calculated sample coverage and the total number of reads mapping to the
718 mitochondrial genome with SAMtools and generated a consensus sequence in FASTA format
719 with ANGSD (V0.933; (Korneliussen et al., 2014).

720 *Subspecies assignment verification.* The subspecies identity of each sample was initially
721 assigned using museum records. We confirmed these assignments using diagnostic sites within
722 the host mitochondrial genome. Using 102 published mitochondrial genomes (Das et al., 2014;
723 Hallast et al., 2016; Hu and Gao, 2016; van der Valk et al., 2018; Xu and Arnason, 1996);
724 Table S12), we identified two sets of diagnostic sites that were fixed for different alleles in
725 each of the contrasted groups using a custom Python script. The first set was species-specific,
726 identifying membership in western versus eastern gorillas. The second set was subspecies-
727 specific, distinguishing between mountain and Grauer's gorillas.

728 *Molecular sexing of samples*. We used sexassign (Gower et al., 2019) to determine the sex of
729 each individual (Table S1). To this end, we mapped filtered reads, prior to removing host and
730 human reads, to the gorilla reference genome (GCF_000151905.2) and counted reads mapping
731 to the X chromosome and the autosomes. sexassign conducts a likelihood ratio test comparing
732 the observed X-to-autosome ratio to expected ratios for males (R_X ~0.5) and females (0.8 > R_X
733 < 1.2).

734 **Initial taxonomic classification and decontamination**

735 *Taxonomic classification with Kraken2/Bracken.* After removing host and human reads, the
736 retained unmapped reads were taxonomically classified using Kraken2 (V2.1.1; Wood et al.,
737 2019) with default parameters. We used the standard Kraken2 database (accessed by the
738 software on 1st September 2021), which includes all bacterial, archaeal and viral genomes from
739 NCBI. Abundances were re-estimated at the species level using Bracken (V2.6.2; Lu et al.,
740 2017), by redistributing reads from higher taxonomic levels to the species level, (setting read
741 length to 55 and the rest of parameters in default). The average read length was set to 55 bp,
742 which corresponded to the average of the mean read length of our data. The raw species table
743 and the corresponding metadata were combined into a phyloseq object (V1.34.0; (McMurdie
744 and Holmes, 2013) in R (V4.0.4; R Core Team, 2015). Taxonomic information was assigned
745 based on taxonomic IDs from the NCBI taxonomy database using the 'classification' function
746 of the taxize package (V0.9.99; (Chamberlain and Szöcs, 2013).

747 *Removal of low-quality samples and contaminant taxa.* Samples containing less than 300,000
748 processed reads were excluded from downstream analysis (for the distribution of read counts
749 per sample see Figure S11). We then evaluated the composition of the microbial communities
750 of the retained samples with FEAST (V0.1.0; Shenhav et al., 2019) using default parameters.

751 FEAST makes use of user-provided reference microbiomes to partition the composition of the
752 study samples and to estimate the proportional contribution of the reference "sources". We
753 provided 29 such sources sampled from six different environments that were chosen to reflect
754 both the oral cavity and potential contaminants. Specifically, we included human calculus (n=5;
755 Mann et al., 2018) and human plaque (n=5; Human Microbiome Project Consortium, 2012;
756 Lloyd-Price et al., 2017) as oral sources, and human gut (n=5; Human Microbiome Project
757 Consortium, 2012; Lloyd-Price et al., 2017), human skin (n=5; Oh et al., 2014), tundra soil
758 (n=5; Johnston et al., 2016) and laboratory contaminants excluding human sequences (n=4;
759 Salter et al., 2014) as potential contaminants (Table S13). Gorilla dental calculus samples for
760 which the proportion of the metagenomic community similar to the human oral microbiome
761 (human calculus and human plaque considered jointly) was lower than 3%, according to the
762 output of FEAST, were excluded from further analyses. The threshold was decided based on
763 the distribution of the oral proportions in the study samples (Figure S3b).

764 For the retained samples, we then carried out a multi-step approach to remove putative
765 contaminant microbial taxa. First, we used the R package decontam (V1.10.0; Davis et al.,
766 2018) with the 'isContaminant' function (method="combined", normalize = TRUE). The
767 package employs two main approaches: a prevalence-based approach, which identifies
768 contaminants based on their increased prevalence in blanks, and a frequency-based approach,
769 which relies on the observation of a reverse relationship between taxon abundance and DNA
770 quantity in the sample. We used a combination of both decontamination approaches, performed
771 separately for the subset of newly generated data, which also included two previously published
772 samples processed in the same facility (Uppsala University, Sweden; Brealey et al., 2020), and
773 data from gorilla dental calculus published by Fellows Yates et al. (2021) and processed at the
774 Max Planck Institute for the Science of Human History, Germany. We refer to these datasets

775 as ‘newly generated’ and Fellows Yates et al. (2021), respectively. Thresholds were allowed
776 to differ by dataset (0.2 for newly generated and 0.3 for Fellows Yates et al. (2021)) and
777 selected to minimise the number of oral taxa (taxa reported as oral in Chen et al. (2010) and
778 Fellows Yates et al. (2021)) among all taxa identified as contaminants (Figure S12). All taxa
779 identified as contaminants were then removed from the full dataset, regardless of which subset
780 they were identified in.

781 Second, we performed abundance filtering on the entire dataset, setting each taxon to 0 if it had
782 relative abundance <0.005% in a given sample. We chose this threshold, as it retained the
783 highest number and proportion of oral taxa, while excluding known contaminant taxa (Table
784 S2). Third, we considered the relative abundances of taxa in the museum controls to remove
785 likely environmental contaminants. A microbial taxon was removed as a likely contaminant if
786 it was found to have a higher relative abundance in at least one of the four museum controls
787 than in any of the samples. Finally, we considered bacterial genera identified as common
788 contaminants in typical molecular and specialised ancient DNA laboratories (Salter et al., 2014;
789 Weyrich et al., 2019). Some of the listed genera included taxa found in the Human Oral
790 Microbiome Database (HOMD; accessed July 14 2021; (Chen et al., 2010) and in the core
791 hominid oral microbiome (Fellows Yates et al., 2021). Therefore, we used a two-step approach
792 to remove these potential contaminant taxa. We directly removed genera that were listed only
793 as contaminants and did not appear in the oral databases. Taxa that were present in both
794 contaminant lists and the oral databases and had a sufficient number of reads in our dataset
795 were investigated further by running mapDamage2 (V2.0.9; Jónsson et al., 2013). To this end,
796 we identified the sample with the highest abundance of a given taxon (according to Kraken2
797 output, requiring at least 10,000 reads) and mapped the reads to the respective reference
798 genome. Taxa with too few reads to be tested were automatically retained. Since many taxa

799 needed to be investigated in this way, making a visual inspection impractical, we assessed the
800 presence of damage using a custom R script (Data and Materials). The presence of typical
801 post-mortem DNA damages was assumed if deamination (C-to-T in the 3' end and G-to-A in
802 the 5' end) was the most frequent change for at least two of the three terminal positions for
803 each fragment end and had the frequency above 0.02 for at least one position. This rule was
804 employed because in-line barcodes can create atypical DNA damage patterns in metagenomic
805 data, showing lower damage at 1st terminal position (Brealey et al., 2020). Bacterial taxa with
806 no damage were assumed to be modern contaminants and were therefore removed. The
807 resulting dataset was used for downstream taxonomic analyses.

808 *Sequence-level decontamination.* We applied additional filtering by removing sequencing
809 reads from taxa identified as contaminants (n=167) to allow for functional characterization of
810 microbial communities and reconstructing metagenome-assembled genomes (MAGs). To this
811 end, we used two approaches. First, we removed reads assigned to contaminants using the
812 'extract_kraken_reads.py' script from the KrakenTools suite (V1.2; Wood et al., 2019). Using
813 the read-level taxonomic assignments by Kraken2, we removed reads assigned to the 167
814 contaminant taxa identified above. This approach retained sequencing reads of all taxa not
815 identified as contaminants (i.e. those included in the final taxonomic dataset), but also a large
816 number of unclassified reads.

817 The reads which remained unclassified by Kraken2 could contain reads belonging to
818 contaminant taxa. Therefore, we performed a further decontamination step. We constructed a
819 dataset containing the genomes of the identified contaminant taxa and a selection of abundant
820 non-contaminant taxa from our dataset. To identify non-contaminant taxa, we selected all taxa
821 with more than 10,000 reads in at least one sample (as long as they were not identified as

822 contaminants), for a total of 72 unique taxa. The non-contaminant taxa were included to avoid
823 forcing the reads to map to the contaminants. For both contaminants and non-contaminants,
824 one genome per taxon was selected from the NCBI assembly summary files for bacteria,
825 archaea, and viruses (NCBI ftp accessed 14 April 2021, available at
826 https://github.com/markella-moraitou/Gorilla_dental_calculus/RD2_mapping/) with the
827 following order of priority: genome representation (full > partial), RefSeq (yes > no), assembly
828 level (full > chromosome > scaffold > contig), publication date (most recent). Twenty
829 contaminant, and 11 non-contaminant taxa did not have a reference genome available in NCBI
830 assembly. For them, we obtained a different genome from the same genus, unless that genus
831 was already represented, using the taxize R package, and selected one genome per missing
832 taxon as a replacement.

833 Finally, all references (consisting of 155 contaminant genomes and 61 non-contaminant
834 genomes) were concatenated into a combined database. We mapped the FASTQ files from the
835 previous decontamination step to this combined reference using BWA-MEM with default
836 settings and then used SAMtools to retain the unmapped reads and reads that mapped primarily
837 to the non-contaminant genomes.

838 **Taxonomic analyses**

839 All taxonomic analyses were performed at the species level. To account for the compositional
840 nature of the data, a centred-log ratio (CLR) normalisation was applied (Gloor et al., 2017)
841 using the 'transform' function of the microbiome R package (V1.12.0; Lahti and Shetty, 2018).

842 *Oral composition.* To assess differences in oral microbiome composition by subspecies and
843 sex, we used two distance measures: Jaccard distances (Jaccard, 1901), which only consider

844 presence-absence of taxa, and Aitchison's distances (Aitchison and Aitchison, 1986), which
845 also take into account relative abundances and are calculated as Euclidean distances on the
846 CLR-transformed data. We performed PERMANOVAs using these two distance metrics by
847 applying the 'adonis' function of the vegan package (V2.5-7; Oksanen et al., 2011) and setting
848 the parameter 'method' to 'jaccard' and 'euclidean' for the non-normalised and normalised
849 data, respectively. Because of the unequal distribution of host subspecies among the two
850 datasets (newly generated versus Fellows Yates et al. (2021); Figure S1), we included dataset
851 as a factor in each model and considered it prior to evaluating the contribution of biological
852 variables. We used the 'adonis.pair' function of the EcolUtils R package (V0.1; Salazar, 2019)
853 to perform pairwise PERMANOVAs for significant factors using Jaccard and Aitchison
854 distance matrices produced with the 'vegdist' function of the vegan package. Principal
855 Coordinate Analysis (PCoA) plots were generated using the 'plot_ordination' function of the
856 phyloseq package. Because sex assignment was missing for some samples (Table S1), we re-
857 ran PERMANOVAs for each distance measure for the subset of samples that could be sexed.

858 *Alpha diversity.* We used the 'estimate_richness' function of the phyloseq package to estimate
859 alpha diversity with two different metrics, applied to the non-normalized data: the Chao1
860 estimator (Chao et al., 2009), which evaluates species richness while accounting for the number
861 of species that are missing from the dataset, and the Shannon index (Shannon, 1948), which
862 reflects evenness. To assess the effect of the host subspecies on alpha diversity, we ran an
863 ANOVA model and confirmed the model met assumptions of normality, using a Shapiro-
864 Wilk's test on the Studentized residuals, and visually assessed the fit against the residuals
865 (Quinn and Keough, 2002). Both Chao1 and Shannon models were transformed to account for
866 skew ('sqrt(500-x)' and 'exp(x)', respectively). Finally, we used a Tukey post-hoc test to
867 compare the different levels of the factor(s) that were statistically significant.

868 *Identification of differentially abundant taxa.* We identified bacterial taxa that significantly
869 differed in abundance between host subspecies using ANCOM-II (Mandal et al., 2015), a
870 method appropriate for compositional data, which accounts for the sparsity of the taxon table
871 (Kaul et al., 2017). To account for the association between host subspecies and dataset (newly
872 generated versus Fellows Yates *et al.* (2021); Figure S1) and to reduce the possibility that we
873 identify dataset-specific taxa as differentially abundant, we ran the analysis twice. First, we
874 identified microbial taxa that differed in abundance between host subspecies, while accounting
875 for read depth. Second, we identified microbial taxa that differed in abundance between
876 datasets, while accounting for the host subspecies. Only genera that differed among subspecies
877 and did not differ by dataset were considered relevant for evaluating microbiome differences
878 among gorilla subspecies. Differentially abundant taxa were identified as those above the 0.9
879 quantile of the ANCOM W-statistic and Kruskal-Wallace post-hoc test (Bonferroni adjusted
880 p-values < 0.05), or those that were structurally absent from one or more subspecies. Only
881 microbial taxa identified at the genus or species level were considered.

882 Following this procedure, we also used ANCOM to identify taxa that differed in abundance
883 between mountain and western lowland gorillas, for both microbial and dietary taxonomic
884 datasets. These taxa were then used to explore the effects of altitude, separating Grauer's
885 gorillas into high- and low-altitude populations and performing comparisons using both
886 Jaccard and Aitchison distances in pairwise PERMANOVAs, in which differences in dataset
887 identity were included as factors.

888 **Functional analysis**

889 Decontaminated metagenomic reads were functionally characterised using an assembly-free
890 approach implemented in the HUMAnN2 pipeline (V0.11.2; Franzosa et al., 2018) using the

891 MetaPhlAn2, UniRef50, and ChocoPhlAn databases (Segata et al., 2012; Truong et al., 2015).
892 The output tables containing the abundances of gene families with specific function were
893 regrouped to show gene ontology (GO) terms (Ashburner et al., 2000; Gene Ontology
894 Consortium, 2021), normalised to copies per million reads and feature abundances across taxa
895 were aggregated in a single feature table, which was imported into R for further analysis. We
896 subset our dataset to GO terms referring to biological processes and used PERMANOVA on
897 their Euclidean distances to investigate functional differences of the oral microbiome by host
898 subspecies. We then compared the abundances of biological processes among host subspecies
899 using ANCOM, using the same approach as above.

900 **Metagenome-assembled genomes (MAGs)**

901 We used the metaWRAP pipeline (V1.3.2; Uritskiy et al., 2018) to construct MAGs from
902 decontaminated sequencing reads. To increase the amount of data available for building the
903 initial assemblies with MEGAHIT (Li et al., 2016), we concatenated the reads across all
904 samples. The initial assembly was split into genomic bins using three different metagenomic
905 binning tools (metabat2; V2.9.1 (Kang et al., 2019), maxbin2; V2 2.2.4 (Wu et al., 2016),
906 CONCOCT; V0.4.0 (Alneberg et al., 2013)) and we retained only those bins that were
907 consistently defined by all three tools. For each MAG, we assigned taxonomic identity with
908 GTDB-TK (Chaumeil et al., 2019) and constructed a phylogeny containing our MAGs and
909 closely-related reference genomes identified by GTDB-TK. The abundance of MAGs in each
910 sample was estimated using salmon (V0.13.1; Patro et al., 2017) and the CLR-transformed
911 abundances were visualised using pheatmap (Kolde and Others, 2012). For each assembled
912 and taxonomically identified MAG, we extracted and curated records of isolation sources
913 (sources listed in Table S8) following an approach described by Madin et al. (2020). This

914 information was used to categorise the isolation sources for taxa into one of the following
915 categories: “contaminant”, “environmental”, “host-associated”, “oral”, or “unknown”.

916 To evaluate evolutionary relationships for select MAGs, reference genomes or gene sequences
917 for the identified species/genus were downloaded from GenBank and Genome Taxonomy
918 Database (GTDB; V202; (Parks et al., 2018). We created alignments using the amino acid
919 sequences of core genes with PhyloPhlAn (V.3.0.2; Segata et al., 2013) and constructed
920 maximum-likelihood phylogenies using FastTree (V2.1.10; Price et al., 2010), which we
921 visualised using ggtree (V3.1.0; Yu et al., 2017).

922 We used two different approaches to determine the presence of genes involved in the nitrate
923 reduction pathway in MAGs belonging to oral genera with nitrate reduction ability (see
924 references provided in Rosier et al. (2020)). First, we used the pangenomic tool Panaroo
925 (Tonkin-Hill et al., 2020) to determine presence of genes across a set of fragmented MAG
926 assemblies. Second, we performed a translated BLAST search (tblastn, V2.11.0; Camacho et
927 al., 2009) using protein sequences obtained from UniProt against MAG contigs. Genes in
928 MAGs and reference genomes were considered as present if detected with either method.

929 **Estimating ecological variation in oral microbiome composition**

930 Using altitude as a proxy for ecology and diet, we estimated the correlation between altitudinal,
931 geographical and microbiome distances. First, we approximated altitude and geographic
932 location (latitude, and longitude) for each specimen based on the collection locality as retrieved
933 from museum records. We constructed Euclidean distance matrices for altitudinal and
934 geographical distance using R package vegan. Using the ade4 R package (1.7-16; Dray et al.,
935 2007), we performed partial Mantel tests (10,000 permutations) between microbiome distance

936 matrices (Pearson correlation used for Jaccard distances and Spearman's rank coefficient
937 correlation for Aitchison taxonomic and Euclidean functional distances) and altitudinal
938 distances, while accounting for the effect of log-transformed geographical distances.

939 To further investigate the effects of altitude on Grauer's gorilla microbiomes, which is the
940 subspecies with the largest altitudinal range (Plumptre et al., 2016), we grouped the Grauer's
941 gorilla samples into low- (500-1000 m above sea level [masl]) and high-altitude (>1000 masl)
942 populations. We evaluated the contribution of altitude by performing a PERMANOVA, after
943 accounting for potential dataset and host subspecies effects. Post hoc tests were performed
944 using pairwise PERMANOVA, as described above.

945 **Dietary Analysis**

946 Eukaryotic reads in dental calculus were used to identify taxa potentially consumed by gorillas.
947 Before taxonomically classifying these reads, we removed reads assigned to prokaryotes and
948 viruses from the metagenomic dataset using the 'extract_kraken_reads.py' script from
949 KrakenTools. The resulting FASTQ files were used as input in a second run of Kraken2 using
950 the NCBI 'nt' database (accessed 27 September 2021). A joint feature table containing species
951 and genus-level assignments was produced using kraken-biom and imported into R for further
952 analysis. The genome coverage for these taxonomic classifications was insufficient for
953 verification using mapDamage2.

954 *Preprocessing of feature table.* The feature table produced by kraken-biom was used in a
955 phyloseq object along with a corresponding taxonomic matrix, created using the taxize R
956 package. Using this matrix, we aggregated all identified taxa to the genus level, and used the
957 decontam (V.1.10.0; Davis et al., 2018) R package to remove likely contaminants, as described

958 above for the oral microbiome analyses, including using different cut-offs for each dataset.
959 Then, all genera present in the museum controls or with fewer than 10 reads per sample were
960 removed, to reduce contaminants, spurious and unreliable classifications. Despite this filtering,
961 spurious classifications or contaminants were still present (species that are unlikely to be
962 consumed by gorillas, e.g. mollusks), so we restricted it to genera belonging to taxonomic
963 families that were previously reported to be consumed by gorillas (Michel et al., 2022; Remis
964 et al., 2001; Rogers et al., 2004; Rothman et al., 2014; Yamagiwa et al., 2005). Since only few
965 reference genomes of tropical plants are available and classically-used barcoding genes
966 represent only a small part of the genome, accurate taxonomic classification from a sparse
967 metagenomic sample is difficult and can likely only be achieved on genus or family level
968 (Mann et al., 2020). For this reason, we focused our analysis not only on genera known to be
969 consumed by gorillas, but also included all detected genera in the same family. The resulting
970 feature table was used to detect differentially abundant dietary components with ANCOM
971 using the same approach as described above, while accounting for differences in the number
972 of reads per sample.

973 *Collecting gorilla diet reference data.* We produced a reference dataset of gorilla foods (Table
974 S11) by searching the literature for plant species known to be consumed by the three gorilla
975 subspecies based either on direct observations, analyses of food remains and faeces or more
976 recently on molecular evidence (Michel et al., 2022; Remis et al., 2001; Rogers et al., 2004;
977 Rothman et al., 2014; Yamagiwa et al., 2005). We retrieved the corresponding taxonomic IDs
978 from NCBI using the taxize R package. For the taxa that had no match in the NCBI Taxonomy
979 database, we manually searched the database and corrected the names that were obviously
980 misspelt (difference of 1-2 characters from the NCBI entry). For the remaining taxa, we
981 manually searched the GBIF species database (Wheeler, 2004) and obtained GBIF taxonomic

982 IDs. However, several taxa (26 out of 314) could not be found in either database and therefore
983 were excluded from our analysis. The taxonomic IDs obtained from either NCBI or GBIF were
984 used with the 'classification' function of taxize to obtain the genus and family name for each
985 taxon.

986 Availability of Data and Materials

987 Sequencing data generated in this study have been deposited on ENA, under Project Accession
988 Number: PRJEB49638. Scripts for both preprocessing and downstream analysis are available
989 at 10.5281/zenodo.6861585.

990

991 Funding

992 This work was supported by the Swedish Research Council (Formas) grant 2019-00275 and
993 the Science for Life Laboratory National Sequencing Projects grant (NP00039) to KG. AF was
994 supported by the Carl Tryggers Stiftelse grant 19:123. JAFY and CW were supported by the
995 Max Planck Society and the Werner Siemens-Stiftung (Paleobiotechnology, awarded to CW).
996 None of the funders had any role in study design, collection, analysis, and interpretation of data
997 and in writing the manuscript.

998

999 Authors' contributions

1000 JCB, MM, AF extracted and prepared genomic libraries for the newly generated data. MM
1001 processed sequencing data, performed bioinformatic and statistical analyses (microbiome

1002 taxonomic and functional analyses, dietary and host genome analyses, altitudinal analyses) and
1003 wrote the manuscript draft. AF performed bioinformatic and statistical analyses (metagenome-
1004 assembled genomes, functional analyses, altitudinal analyses), wrote the respective parts of the
1005 manuscript and contributed to others. JCB performed initial bioinformatics analyses on a
1006 smaller dataset. JAFY and CW provided genomic data. KG conceived the research plan,
1007 interpreted the results, provided financial support and infrastructure, and contributed
1008 significantly to manuscript writing. All authors contributed to writing the final version of this
1009 manuscript.

1010

1011 **Acknowledgments**

1012 We would like to thank Henrique Leitão, Thijs Hofstede, Franziska Aron, and Cody Parker,
1013 who contributed with processing the samples in the ancient DNA lab, Tom van der Valk, Axel
1014 Jensen and Samantha López Clinton for their contribution to subspecies verification using
1015 mitochondrial DNA. We thank Daniela C. Kalthoff at the Swedish Museum of Natural History,
1016 Emmanuel Gilissen at the Royal Museum for Central Africa, Tom Geerinckx and Patrick
1017 Semal at the Royal Belgian Institute of Natural Sciences, and Lyman Jellema at the Cleveland
1018 Museum of Natural History for providing access to and assistance with the gorilla specimens.
1019 Sequencing was performed by the SNP&SEQ Technology Platform in Uppsala. The
1020 SNP&SEQ Technology Platform is part of the National Genomics Infrastructure Sweden and
1021 Science of Life Laboratory. The SNP&SEQ Platform is also supported by the Swedish
1022 Research Council and the Knut and Alice Wallenberg Foundation. We also acknowledge the
1023 National Bioinformatics Infrastructure for providing computational resources to this project.

References

Abusleme L, Dupuy AK, Dutzan N, Silva N, Burleson JA, Strausbaugh LD, Gamonal J, Diaz PI. 2013. The subgingival microbiome in health and periodontitis and its relationship with community biomass and inflammation. *ISME J* **7**:1016–1025. doi:10.1038/ismej.2012.174

Abusleme L, O'Gorman H, Dutzan N, Greenwell-Wild T, Moutsopoulos NM. 2020. Establishment and Stability of the Murine Oral Microbiome. *J Dent Res* **99**:721–729. doi:10.1177/0022034520915485

Adler CJ, Dobney K, Weyrich LS, Kaidonis J, Walker AW, Haak W, Bradshaw CJA, Townsend G, Sołtysiak A, Alt KW, Parkhill J, Cooper A. 2013. Sequencing ancient calcified dental plaque shows changes in oral microbiota with dietary shifts of the Neolithic and Industrial revolutions. *Nat Genet* **45**:450–5, 455e1. doi:10.1038/ng.2536

Adler CJ, Malik R, Browne GV, Norris JM. 2016. Diet may influence the oral microbiome composition in cats. *Microbiome* **4**:23. doi:10.1186/s40168-016-0169-y

Aitchison J, Aitchison JW. 1986. The Statistical Analysis of Compositional Data. Springer Netherlands.

Alberdi A, Aizpurua O, Bohmann K, Zepeda-Mendoza ML, Gilbert MTP. 2016. Do Vertebrate Gut Metagenomes Confer Rapid Ecological Adaptation? *Trends Ecol Evol* **31**:689–699. doi:10.1016/j.tree.2016.06.008

Alneberg J, Bjarnason BS, de Bruijn I, Schirmer M, Quick J, Ijaz UZ, Loman NJ, Andersson AF, Quince C. 2013. CONCOCT: Clustering cONtigs on COverage and ComposiTion. *arXiv [q-bioGN]*.

Anderson MJ. 2001. A new method for non-parametric multivariate analysis of variance. *Austral Ecol* **26**:32–46. doi:10.1111/j.1442-9993.2001.01070.pp.x

Arora T, Sharma R. 2011. Fermentation potential of the gut microbiome: implications for energy homeostasis and weight management. *Nutr Rev* **69**:99–106. doi:10.1111/j.1753-4887.2010.00365.x

Ashburner M, Ball CA, Blake JA, Botstein D, Butler H, Michael Cherry J, Davis AP, Dolinski K, Dwight SS, Eppig JT, Harris MA, Hill DP, Issel-Tarver L, Kasarskis A, Lewis S, Matese JC, Richardson JE, Ringwald M, Rubin GM, Sherlock G. 2000. Gene Ontology: tool for the unification of biology. *Nature Genetics*. doi:10.1038/75556

Beall CM, Laskowski D, Erzurum SC. 2012. Nitric oxide in adaptation to altitude. *Free Radic Biol Med* **52**:1123–1134. doi:10.1016/j.freeradbiomed.2011.12.028

Beall CM, Laskowski D, Strohl KP, Soria R, Villena M, Vargas E, Alarcon AM, Gonzales C, Erzurum SC. 2001. Pulmonary nitric oxide in mountain dwellers. *Nature* **414**:411–412. doi:10.1038/35106641

Boehlke C, Rupf S, Tenniswood M, Chittur SV, Hannig C, Zierau O. 2020. Caries and periodontitis associated bacteria are more abundant in human saliva compared to other great apes. *Arch Oral Biol* **111**:104648. doi:10.1016/j.archoralbio.2020.104648

Bo T-B, Zhang X-Y, Kohl KD, Wen J, Tian S-J, Wang D-H. 2020. Coprophagy prevention alters microbiome, metabolism, neurochemistry, and cognitive behavior in a small mammal. *The ISME Journal*. doi:10.1038/s41396-020-0711-6

Brealey JC, Leitão HG, Hofstede T, Kalthoff DC, Guschanski K. 2021. The oral microbiota of wild bears in Sweden reflects the history of antibiotic use by humans. *Curr Biol* **31**:4650–4658.e6. doi:10.1016/j.cub.2021.08.010

Brealey JC, Leitão HG, van der Valk T, Xu W, Bougiouri K, Dalén L, Guschanski K. 2020. Dental Calculus as a Tool to Study the Evolution of the Mammalian Oral Microbiome.

Mol Biol Evol **37**:3003–3022. doi:10.1093/molbev/msaa135
Briggs AW, Stenzel U, Johnson PLF, Green RE, Kelso J, Prüfer K, Meyer M, Krause J, Ronan MT, Lachmann M, Pääbo S. 2007. Patterns of damage in genomic DNA sequences from a Neandertal. *Proc Natl Acad Sci U S A* **104**:14616–14621. doi:10.1073/pnas.0704665104
Bryan NS, Tribble G, Angelov N. 2017. Oral Microbiome and Nitric Oxide: the Missing Link in the Management of Blood Pressure. *Curr Hypertens Rep* **19**:33. doi:10.1007/s11906-017-0725-2
Bushnell B. 2014. BBMap: A fast, accurate, splice-aware aligner (No. LBNL-7065E). Lawrence Berkeley National Lab. (LBNL), Berkeley, CA (United States).
Camacho C, Coulouris G, Avagyan V, Ma N, Papadopoulos J, Bealer K, Madden TL. 2009. BLAST+: architecture and applications. *BMC Bioinformatics* **10**:421. doi:10.1186/1471-2105-10-421
Cephas KD, Kim J, Mathai RA, Barry KA, Dowd SE, Meline BS, Swanson KS. 2011. Comparative Analysis of Salivary Bacterial Microbiome Diversity in Edentulous Infants and Their Mothers or Primary Care Givers Using Pyrosequencing. *PLoS ONE*. doi:10.1371/journal.pone.0023503
Chamberlain SA, Szöcs E. 2013. taxize: taxonomic search and retrieval in R. *F1000Res* **2**:191. doi:10.12688/f1000research.2-191.v2
Chao A, Colwell RK, Lin C-W, Gotelli NJ. 2009. Sufficient sampling for asymptotic minimum species richness estimators. *Ecology* **90**:1125–1133. doi:10.1890/07-2147.1
Chaumeil P-A, Mussig AJ, Hugenholtz P, Parks DH. 2019. GTDB-Tk: a toolkit to classify genomes with the Genome Taxonomy Database. *Bioinformatics*. doi:10.1093/bioinformatics/btz848
Chen S, Zhou Y, Chen Y, Gu J. 2018. fastp: an ultra-fast all-in-one FASTQ preprocessor. *Bioinformatics* **34**:i884–i890. doi:10.1093/bioinformatics/bty560
Chen T, Yu W-H, Izard J, Baranova OV, Lakshmanan A, Dewhirst FE. 2010. The Human Oral Microbiome Database: a web accessible resource for investigating oral microbe taxonomic and genomic information. *Database* **2010**:baq013. doi:10.1093/database/baq013
Cobb CM, Kelly PJ, Williams KB, Babbar S, Angolkar M, Derman RJ. 2017. The oral microbiome and adverse pregnancy outcomes. *Int J Womens Health* **9**:551–559. doi:10.2147/IJWH.S142730
Corby PM, Bretz WA, Hart TC, Schork NJ, Wessel J, Lyons-Weiler J, Paster BJ. 2007. Heritability of oral microbial species in caries-active and caries-free twins. *Twin Res Hum Genet* **10**:821–828. doi:10.1375/twin.10.6.821
Dabney J, Knapp M, Glocke I, Gansauge M-T, Weihmann A, Nickel B, Valdiosera C, García N, Pääbo S, Arsuaga J-L, Meyer M. 2013. Complete mitochondrial genome sequence of a Middle Pleistocene cave bear reconstructed from ultrashort DNA fragments. *Proc Natl Acad Sci U S A* **110**:15758–15763. doi:10.1073/pnas.1314445110
Dabney J, Meyer M. 2012. Length and GC-biases during sequencing library amplification: a comparison of various polymerase-buffer systems with ancient and modern DNA sequencing libraries. *Biotechniques* **52**:87–94. doi:10.2144/000113809
Danecek P, Bonfield JK, Liddle J, Marshall J, Ohan V, Pollard MO, Whitwham A, Keane T, McCarthy SA, Davies RM, Li H. 2021. Twelve years of SAMtools and BCFtools. *Gigascience* **10**. doi:10.1093/gigascience/giab008
Das R, Hergenrother SD, Soto-Calderón ID, Dew JL, Anthony NM, Jensen-Seaman MI. 2014. Complete mitochondrial genome sequence of the Eastern gorilla (Gorilla beringei)

and implications for african ape biogeography. *J Hered* **105**:752–761. doi:10.1093/jhered/esu056

Davis NM, Proctor DM, Holmes SP, Relman DA, Callahan BJ. 2018. Simple statistical identification and removal of contaminant sequences in marker-gene and metagenomics data. *Microbiome* **6**:226. doi:10.1186/s40168-018-0605-2

Delamuta JRM, Scherer AJ, Ribeiro RA, Hungria M. 2020. Genetic diversity of Agrobacterium species isolated from nodules of common bean and soybean in Brazil, Mexico, Ecuador and Mozambique, and description of the new species Agrobacterium fabacearum sp. nov. *Int J Syst Evol Microbiol* **70**:4233–4244. doi:10.1099/ijsem.0.004278

Dominguez-Bello MG, Costello EK, Contreras M, Magris M, Hidalgo G, Fierer N, Knight R. 2010. Delivery mode shapes the acquisition and structure of the initial microbiota across multiple body habitats in newborns. *Proc Natl Acad Sci U S A* **107**:11971–11975. doi:10.1073/pnas.1002601107

Donati C, Zolfo M, Albanese D, Tin Truong D, Asnicar F, Iebba V, Cavalieri D, Jousson O, De Filippo C, Huttenhower C, Segata N. 2016. Uncovering oral Neisseria tropism and persistence using metagenomic sequencing. *Nat Microbiol* **1**:16070. doi:10.1038/nmicrobiol.2016.70

Doran DM, McNeilage A, Greer D, Bocian C, Mehlman P, Shah N. 2002. Western lowland gorilla diet and resource availability: new evidence, cross-site comparisons, and reflections on indirect sampling methods. *Am J Primatol* **58**:91–116. doi:10.1002/ajp.10053

Dray S, Dufour A-B, Others. 2007. The ade4 package: implementing the duality diagram for ecologists. *J Stat Softw* **22**:1–20.

Eriksson H, Bagge E, Båverud V, Fellström C, Jansson DS. 2014. Erysipelothrix rhusiopathiae contamination in the poultry house environment during erysipelas outbreaks in organic laying hen flocks. *Avian Pathol* **43**:231–237. doi:10.1080/03079457.2014.907485

Erzurum SC, Ghosh S, Janocha AJ, Xu W, Bauer S, Bryan NS, Tejero J, Hemann C, Hille R, Stuehr DJ, Feelisch M, Beall CM. 2007. Higher blood flow and circulating NO products offset high-altitude hypoxia among Tibetans. *Proc Natl Acad Sci U S A* **104**:17593–17598. doi:10.1073/pnas.0707462104

Feelisch M. 2018. Enhanced nitric oxide production is a universal response to hypoxic stress. *National Science Review*. doi:10.1093/nsr/nwy041

Fellows Yates JA, Velsko IM, Aron F, Posth C, Hofman CA, Austin RM, Parker CE, Mann AE, Nägele K, Arthur KW, Arthur JW, Bauer CC, Crevecoeur I, Cupillard C, Curtis MC, Dalén L, Díaz-Zorita Bonilla M, Díez Fernández-Lomana JC, Drucker DG, Escribano Escrivá E, Francken M, Gibbon VE, González Morales MR, Grande Mateu A, Harvati K, Henry AG, Humphrey L, Menéndez M, Mihailović D, Peresani M, Rodríguez Moroder S, Roksandic M, Rougier H, Sázelová S, Stock JT, Straus LG, Svoboda J, Teßmann B, Walker MJ, Power RC, Lewis CM, Sankaranarayanan K, Guschanski K, Wrangham RW, Dewhirst FE, Salazar-García DC, Krause J, Herbig A, Warinner C. 2021. The evolution and changing ecology of the African hominid oral microbiome. *Proc Natl Acad Sci U S A* **118**. doi:10.1073/pnas.2021655118

Fletcher A, Nowell A. 2008. The development of feeding behaviour in wild western lowland gorillas (Gorilla gorilla gorilla). *Behaviour*. doi:10.1163/156853907783244747

Flynn KJ, Baxter NT, Schloss PD. 2016. Metabolic and Community Synergy of Oral Bacteria in Colorectal Cancer. *mSphere* **1**. doi:10.1128/mSphere.00102-16

1167 Franzosa EA, McIver LJ, Rahnavard G, Thompson LR, Schirmer M, Weingart G, Lipson KS,
1168 Knight R, Caporaso JG, Segata N, Huttenhower C. 2018. Species-level functional
1169 profiling of metagenomes and metatranscriptomes. *Nat Methods* **15**:962–968.
1170 doi:10.1038/s41592-018-0176-y
1171 Galbany J, Imanizabayo O, Romero A, Vecellio V, Glowacka H, Cranfield MR, Bromage
1172 TG, Mudakikwa A, Stoinski TS, McFarlin SC. 2016. Tooth wear and feeding ecology in
1173 mountain gorillas from Volcanoes National Park, Rwanda. *Am J Phys Anthropol*
1174 **159**:457–465. doi:10.1002/ajpa.22897
1175 Ganas J, Robbins MM, Nkurunungi JB, Kaplin BA, McNeilage A. 2004. Dietary variability
1176 of mountain gorillas in bwindi impenetrable National Park, Uganda. *Int J Primatol*
1177 **25**:1043–1072. doi:10.1023/b:ijop.0000043351.20129.44
1178 Gao S, Li S, Ma Z, Liang S, Shan T, Zhang M, Zhu X, Zhang P, Liu G, Zhou F, Yuan X, Jia
1179 R, Potempa J, Scott DA, Lamont RJ, Wang H, Feng X. 2016. Presence of
1180 Porphyromonas gingivalis in esophagus and its association with the clinicopathological
1181 characteristics and survival in patients with esophageal cancer. *Infectious Agents and*
1182 *Cancer*. doi:10.1186/s13027-016-0049-x
1183 Gene Ontology Consortium. 2021. The Gene Ontology resource: enriching a GOld mine.
1184 *Nucleic Acids Res* **49**:D325–D334. doi:10.1093/nar/gkaa1113
1185 Gerner-Smidt P, Keiser-Nielsen H, Dorsch M, Stackebrandt E, Ursing J, Blom J, Christensen
1186 AC, Christensen JJ, Frederiksen W, Hoffmann S. 1994. Lautropia mirabilis gen. nov.,
1187 sp. nov., a gram-negative motile coccus with unusual morphology isolated from the
1188 human mouth. *Microbiology* **140 (Pt 7)**:1787–1797. doi:10.1099/13500872-140-7-1787
1189 Gloor GB, Macklaim JM, Pawlowsky-Glahn V, Egozcue JJ. 2017. Microbiome Datasets Are
1190 Compositional: And This Is Not Optional. *Front Microbiol* **8**:2224.
1191 doi:10.3389/fmicb.2017.02224
1192 Gower G, Fenderson LE, Salis AT, Helgen KM, van Loenen AL, Heiniger H, Hofman-
1193 Kamińska E, Kowalczyk R, Mitchell KJ, Llamas B, Cooper A. 2019. Widespread male
1194 sex bias in mammal fossil and museum collections. *Proc Natl Acad Sci U S A*
1195 **116**:19019–19024. doi:10.1073/pnas.1903275116
1196 Graczyk TK, Cranfield MR. 2003. Coprophagy and intestinal parasites: implications to
1197 human-habituated mountain gorillas (Gorilla gorilla beringei) of the Virunga Mountains
1198 and Bwindi Impenetrable Forest. *Primate Conserv* **9**:58–64.
1199 Haas FB, Eisenhofer R, Schreiber M, Weyrich LS, Rensing SA. 2022. Neanderthals did not
1200 likely consume Physcomitrium patens – a model moss species.
1201 doi:10.1101/2022.01.26.472964
1202 Hallast P, Maisano Delser P, Batini C, Zadik D, Rocchi M, Schempp W, Tyler-Smith C,
1203 Jobling MA. 2016. Great ape Y Chromosome and mitochondrial DNA phylogenies
1204 reflect subspecies structure and patterns of mating and dispersal. *Genome Res* **26**:427–
1205 439. doi:10.1101/gr.198754.115
1206 Hezel MP, Weitzberg E. 2015. The oral microbiome and nitric oxide homoeostasis. *Oral Dis*
1207 **21**:7–16. doi:10.1111/odi.12157
1208 Human Microbiome Project Consortium. 2012. Structure, function and diversity of the
1209 healthy human microbiome. *Nature* **486**:207–214. doi:10.1038/nature11234
1210 Hu X-D, Gao L-Z. 2016. The complete mitochondrial genome of eastern lowland gorilla,
1211 Gorilla beringei graueri, and comparative mitochondrial genomics of Gorilla species.
1212 *Mitochondrial DNA A DNA Mapp Seq Anal* **27**:1484–1485.
1213 doi:10.3109/19401736.2014.953103
1214 Hyde ER, Andrade F, Vaksman Z, Parthasarathy K, Jiang H, Parthasarathy DK, Torregrossa

AC, Tribble G, Kaplan HB, Petrosino JF, Bryan NS. 2014a. Metagenomic analysis of nitrate-reducing bacteria in the oral cavity: implications for nitric oxide homeostasis. *PLoS One* **9**:e88645. doi:10.1371/journal.pone.0088645

Hyde ER, Luk B, Cron S, Kusic L, McCue T, Bauch T, Kaplan H, Tribble G, Petrosino JF, Bryan NS. 2014b. Characterization of the rat oral microbiome and the effects of dietary nitrate. *Free Radic Biol Med* **77**:249–257. doi:10.1016/j.freeradbiomed.2014.09.017

Jaccard P. 1901. Étude comparative de la distribution florale dans une portion des Alpes et des Jura. *Bull Soc Vaud sci nat* **37**:547–579.

Janiak MC, Montague MJ, Villamil CI, Stock MK, Trujillo AE, DePasquale AN, Orkin JD, Bauman Surratt SE, Gonzalez O, Platt ML, Martínez MI, Antón SC, Dominguez-Bello MG, Melin AD, Higham JP. 2021. Age and sex-associated variation in the multi-site microbiome of an entire social group of free-ranging rhesus macaques. *Microbiome* **9**:68. doi:10.1186/s40168-021-01009-w

Jiao J-Y, Liu L, Hua Z-S, Fang B-Z, Zhou E-M, Salam N, Hedlund BP, Li W-J. 2021. Microbial dark matter coming to light: challenges and opportunities. *Natl Sci Rev* **8**:nwaa280. doi:10.1093/nsr/nwaa280

Johnston ER, Rodriguez-R LM, Luo C, Yuan MM, Wu L, He Z, Schuur EAG, Luo Y, Tiedje JM, Zhou J, Konstantinidis KT. 2016. Metagenomics Reveals Pervasive Bacterial Populations and Reduced Community Diversity across the Alaska Tundra Ecosystem. *Front Microbiol* **7**:579. doi:10.3389/fmicb.2016.00579

Jones AM, Vanhatalo A, Seals DR, Rossman MJ, Piknova B, Jonvik KL. 2021. Dietary Nitrate and Nitric Oxide Metabolism: Mouth, Circulation, Skeletal Muscle, and Exercise Performance. *Med Sci Sports Exerc* **53**:280–294. doi:10.1249/MSS.0000000000002470

Jónsson H, Ginolhac A, Schubert M, Johnson PLF, Orlando L. 2013. mapDamage2.0: fast approximate Bayesian estimates of ancient DNA damage parameters. *Bioinformatics* **29**:1682–1684. doi:10.1093/bioinformatics/btt193

Kang DD, Li F, Kirton E, Thomas A, Egan R, An H, Wang Z. 2019. MetaBAT 2: an adaptive binning algorithm for robust and efficient genome reconstruction from metagenome assemblies. *PeerJ* **7**:e7359. doi:10.7717/peerj.7359

Kartzinel TR, Hsing JC, Musili PM, Brown BRP, Pringle RM. 2019. Covariation of diet and gut microbiome in African megafauna. *Proc Natl Acad Sci U S A* **116**:23588–23593. doi:10.1073/pnas.1905666116

Kaul A, Mandal S, Davidov O, Peddada SD. 2017. Analysis of Microbiome Data in the Presence of Excess Zeros. *Front Microbiol* **8**:2114. doi:10.3389/fmicb.2017.02114

Kolde R, Others. 2012. Pheatmap: pretty heatmaps. *R package version* **1**:726.

Kolenbrander PE, Palmer RJ Jr, Periasamy S, Jakubovics NS. 2010. Oral multispecies biofilm development and the key role of cell-cell distance. *Nat Rev Microbiol* **8**:471–480. doi:10.1038/nrmicro2381

Korneliussen TS, Albrechtsen A, Nielsen R. 2014. ANGSD: Analysis of Next Generation Sequencing Data. *BMC Bioinformatics* **15**:356. doi:10.1186/s12859-014-0356-4

Lahti L, Shetty S. 2018. Introduction to the microbiome R package. http://bioconductor.statistik.tu-dortmund.de/packages/3.6/bioc/vignettes/microbiome/inst/doc/vignette.html

Levett DZ, Fernandez BO, Riley HL, Martin DS, Mitchell K, Leckstrom CA, Ince C, Whipp BJ, Mythen MG, Montgomery HE, Grocott MP, Feelisch M, Caudwell Extreme Everest Research Group. 2011. The role of nitrogen oxides in human adaptation to hypoxia. *Sci Rep* **1**:109. doi:10.1038/srep00109

Levin D, Raab N, Pinto Y, Rothschild D, Zanir G, Godneva A, Mellul N, Futorian D, Gal D,

Leviatan S, Zeevi D, Bachelet I, Segal E. 2021. Diversity and functional landscapes in the microbiota of animals in the wild. *Science* **372**. doi:10.1126/science.abb5352

Li D, Luo R, Liu C-M, Leung C-M, Ting H-F, Sadakane K, Yamashita H, Lam T-W. 2016. MEGAHIT v1.0: A fast and scalable metagenome assembler driven by advanced methodologies and community practices. *Methods* **102**:3–11. doi:10.1016/j.ymeth.2016.02.020

Li H, Durbin R. 2009. Fast and accurate short read alignment with Burrows-Wheeler transform. *Bioinformatics* **25**:1754–1760. doi:10.1093/bioinformatics/btp324

Li J, Nasidze I, Quinque D, Li M, Horz H-P, André C, Garriga RM, Halbwax M, Fischer A, Stoneking M. 2013. The saliva microbiome of Pan and Homo. *BMC Microbiol* **13**:204. doi:10.1186/1471-2180-13-204

Li Y, Ismail AI, Ge Y, Tellez M, Sohn W. 2007. Similarity of Bacterial Populations in Saliva from African-American Mother-Child Dyads. *Journal of Clinical Microbiology*. doi:10.1128/jcm.00771-07

Lloyd-Price J, Mahurkar A, Rahnavard G, Crabtree J, Orvis J, Hall AB, Brady A, Creasy HH, McCracken C, Giglio MG, McDonald D, Franzosa EA, Knight R, White O, Huttenhower C. 2017. Strains, functions and dynamics in the expanded Human Microbiome Project. *Nature* **550**:61–66. doi:10.1038/nature23889

Lu J, Breitwieser FP, Thielen P, Salzberg SL. 2017. Bracken: estimating species abundance in metagenomics data. *PeerJ Comput Sci* **3**:e104. doi:10.7717/peerj-cs.104

Lundberg JO, Carlström M, Weitzberg E. 2018. Metabolic Effects of Dietary Nitrate in Health and Disease. *Cell Metab* **28**:9–22. doi:10.1016/j.cmet.2018.06.007

Madin JS, Nielsen DA, Brbic M, Corkrey R, Danko D, Edwards K, Engqvist MKM, Fierer N, Geoghegan JL, Gillings M, Kyrpides NC, Litchman E, Mason CE, Moore L, Nielsen SL, Paulsen IT, Price ND, Reddy TBK, Richards MA, Rocha EPC, Schmidt TM, Shaaban H, Shukla M, Supek F, Tetu SG, Vieira-Silva S, Wattam AR, Westfall DA, Westoby M. 2020. A synthesis of bacterial and archaeal phenotypic trait data. *Sci Data* **7**:170. doi:10.1038/s41597-020-0497-4

Maisels F, Bergl RA, Williamson EA. 2018. Gorilla gorilla (amended version of 2016 assessment). *The IUCN Red List of Threatened Species* 2018–2012.

Mandal S, Van Treuren W, White RA, Eggesbø M, Knight R, Peddada SD. 2015. Analysis of composition of microbiomes: a novel method for studying microbial composition. *Microbial Ecology in Health & Disease*. doi:10.3402/mehd.v26.27663

Mann AE, Fellows Yates JA, Fagernäs Z, Austin RM, Nelson EA, Hofman CA. 2020. Do I have something in my teeth? The trouble with genetic analyses of diet from archaeological dental calculus. *Quat Int*. doi:10.1016/j.quaint.2020.11.019

Mann AE, Sabin S, Ziesemer K, Vågene ÅJ, Schroeder H, Ozga AT, Sankaranarayanan K, Hofman CA, Fellows Yates JA, Salazar-García DC, Frohlich B, Aldenderfer M, Hoogland M, Read C, Milner GR, Stone AC, Lewis CM Jr, Krause J, Hofman C, Bos KI, Warinner C. 2018. Differential preservation of endogenous human and microbial DNA in dental calculus and dentin. *Sci Rep* **8**:9822. doi:10.1038/s41598-018-28091-9

Marcelino, R, Vanessa, Holmes EC, Sorrell TC. 2020. The use of taxon-specific reference databases compromises metagenomic classification. *BMC Genomics* **21**:184. doi:10.1186/s12864-020-6592-2

Mark Welch JL, Rossetti BJ, Rieken CW, Dewhirst FE, Borisy GG. 2016. Biogeography of a human oral microbiome at the micron scale. *Proceedings of the National Academy of Sciences* **113**:E791–E800.

McManus KF, Kelley JL, Song S, Veeramah KR, Woerner AE, Stevison LS, Ryder OA, Ape

1311 Genome Project G, Kidd JM, Wall JD, Bustamante CD, Hammer MF. 2015. Inference
1312 of gorilla demographic and selective history from whole-genome sequence data. *Mol*
1313 *Biol Evol* **32**:600–612. doi:10.1093/molbev/msu394
1314 McMurdie PJ, Holmes S. 2013. phyloseq: An R Package for Reproducible Interactive
1315 Analysis and Graphics of Microbiome Census Data. *PLoS ONE*.
1316 doi:10.1371/journal.pone.0061217
1317 Meyer M, Kircher M. 2010. Illumina sequencing library preparation for highly multiplexed
1318 target capture and sequencing. *Cold Spring Harb Protoc* **2010**:db.prot5448.
1319 doi:10.1101/pdb.prot5448
1320 Michel A, Minocher R, Niehoff P, Li Y, Nota K, Gadhvi MA, Su J, Iyer N, Porter A,
1321 Ngobobo-As-Ibungu U, Binyinyi E, Pekeyake RN, Parducci L, Caillaud D, Guschanski
1322 K. 2022. Isolated Grauer's gorilla populations differ in diet and gut microbiome.
1323 *bioRxiv*. doi:10.1101/2022.01.04.474987
1324 Moeller AH, Foerster S, Wilson ML, Pusey AE, Hahn BH, Ochman H. 2016. Social behavior
1325 shapes the chimpanzee pan-microbiome. *Sci Adv* **2**:e1500997.
1326 doi:10.1126/sciadv.1500997
1327 Mukherjee S, Huntemann M, Ivanova N, Kyrpides NC, Pati A. 2015. Large-scale
1328 contamination of microbial isolate genomes by Illumina PhiX control. *Stand Genomic*
1329 *Sci* **10**:18. doi:10.1186/1944-3277-10-18
1330 Nakano K, Wada K, Nomura R, Nemoto H, Inaba H, Kojima A, Naka S, Hokamura K,
1331 Mukai T, Nakajima A, Umemura K, Kamisaki Y, Yoshioka H, Taniguchi K, Amano A,
1332 Ooshima T. 2011. Characterization of aortic aneurysms in cardiovascular disease
1333 patients harboring Porphyromonas gingivalis. *Oral Dis* **17**:370–378. doi:10.1111/j.1601-
1334 0825.2010.01759.x
1335 Nearing JT, DeClercq V, Van Limbergen J, Langille MGI. 2020. Assessing the Variation
1336 within the Oral Microbiome of Healthy Adults. *mSphere* **5**.
1337 doi:10.1128/mSphere.00451-20
1338 Nichols RG, Peters JM, Patterson AD. 2019. Interplay Between the Host, the Human
1339 Microbiome, and Drug Metabolism. *Hum Genomics* **13**:27. doi:10.1186/s40246-019-
1340 0211-9
1341 Nieuwdorp M, Gilijamse PW, Pai N, Kaplan LM. 2014. Role of the microbiome in energy
1342 regulation and metabolism. *Gastroenterology* **146**:1525–1533.
1343 doi:10.1053/j.gastro.2014.02.008
1344 Nikitakis NG, Papaioannou W, Sakkas LI, Kousvelari E. 2017. The autoimmunity-oral
1345 microbiome connection. *Oral Dis* **23**:828–839. doi:10.1111/odi.12589
1346 Nishida AH, Ochman H. 2018. Rates of gut microbiome divergence in mammals. *Mol Ecol*
1347 **27**:1884–1897. doi:10.1111/mec.14473
1348 Oh J, Byrd AL, Deming C, Conlan S, NISC Comparative Sequencing Program, Kong HH,
1349 Segre JA. 2014. Biogeography and individuality shape function in the human skin
1350 metagenome. *Nature* **514**:59–64. doi:10.1038/nature13786
1351 Oksanen J, Blanchet FG, Kindt R, Legendre P, Minchin PR, O'hara RB, Simpson GL,
1352 Solymos P, Stevens MHH, Wagner H. 2011. vegan: Community ecology package. *R*
1353 *package version* 117–118.
1354 Olsen I, Singhrao SK. 2015. Can oral infection be a risk factor for Alzheimer's disease? *J*
1355 *Oral Microbiol* **7**:29143. doi:10.3402/jom.v7.29143
1356 Ottoni C, Guellil M, Ozga AT, Stone AC, Kersten O, Bramanti B, Porcier S, Van Neer W.
1357 2019. Metagenomic analysis of dental calculus in ancient Egyptian baboons. *Scientific*
1358 *Reports*. doi:10.1038/s41598-019-56074-x

Ozga AT, Nieves-Colón MA, Honap TP, Sankaranarayanan K, Hofman CA, Milner GR, Lewis CM Jr, Stone AC, Warinner C. 2016. Successful enrichment and recovery of whole mitochondrial genomes from ancient human dental calculus. *Am J Phys Anthropol* **160**:220–228. doi:10.1002/ajpa.22960

Ozga AT, Ottoni C. 2021. Dental calculus as a proxy for animal microbiomes. *Quat Int*. doi:10.1016/j.quaint.2021.06.012

Parks DH, Chuvochina M, Waite DW, Rinke C, Skarshewski A, Chaumeil P-A, Hugenholtz P. 2018. A standardized bacterial taxonomy based on genome phylogeny substantially revises the tree of life. *Nat Biotechnol* **36**:996–1004. doi:10.1038/nbt.4229

Patro R, Duggal G, Love MI, Irizarry RA, Kingsford C. 2017. Salmon provides fast and bias-aware quantification of transcript expression. *Nat Methods* **14**:417–419. doi:10.1038/nmeth.4197

Plumptre A, Nixon S, Caillaud D, Hall JS, Hart JA, Nishuli R, Williamson EA. 2016. Gorilla beringei ssp. graueri. The IUCN Red List of Threatened Species 2016: e. T39995A102328430 DOI 10.2305/IUCN. UK. 2016-2. *RLTS T39995A17989838 en*.

Poole P, Ramachandran V, Terpolilli J. 2018. Rhizobia: from saprophytes to endosymbionts. *Nat Rev Microbiol* **16**:291–303. doi:10.1038/nrmicro.2017.171

Price MN, Dehal PS, Arkin AP. 2010. FastTree 2--approximately maximum-likelihood trees for large alignments. *PLoS One* **5**:e9490. doi:10.1371/journal.pone.0009490

Quinlan AR, Hall IM. 2010. BEDTools: a flexible suite of utilities for comparing genomic features. *Bioinformatics* **26**:841–842. doi:10.1093/bioinformatics/btq033

Quinn GP, Keough MJ. 2002. Experimental Design and Data Analysis for Biologists. doi:10.1017/cbo9780511806384

Radini A, Nikita E, Buckley S, Copeland L, Hardy K. 2017. Beyond food: The multiple pathways for inclusion of materials into ancient dental calculus. *Am J Phys Anthropol* **162 Suppl 63**:71–83. doi:10.1002/ajpa.23147

R Core Team. 2015. R: A Language and Environment for Statistical Computing. Vienna, Austria: R Foundation for Statistical Computing.

Remis MJ, Dierenfeld ES, Mowry CB, Carroll RW. 2001. Nutritional aspects of western lowland gorilla (Gorilla gorilla gorilla) diet during seasons of fruit scarcity at Bai Hokou, Central African Republic. *Int J Primatol* **22**:807–836.

Rogers ME, Abernethy K, Bermejo M, Cipolletta C, Doran D, McFarland K, Nishihara T, Remis M, Tutin CEG. 2004. Western gorilla diet: a synthesis from six sites. *Am J Primatol* **64**:173–192. doi:10.1002/ajp.20071

Rosier BT, Moya-Gonzalvez EM, Corell-Escuin P, Mira A. 2020. Isolation and Characterization of Nitrate-Reducing Bacteria as Potential Probiotics for Oral and Systemic Health. *Front Microbiol* **11**:555465. doi:10.3389/fmicb.2020.555465

Rosier BT, Takahashi N, Zaura E, Krom BP, MartÍnez-Espinosa RM, van Breda SGJ, Marsh PD, Mira A. 2022. The Importance of Nitrate Reduction for Oral Health. *J Dent Res* 220345221080982. doi:10.1177/00220345221080982

Rothman JM, Nkurunungi JB, Shannon BF, Bryer MAH. 2014. High Altitude Diets: Implications for the Feeding and Nutritional Ecology of Mountain Gorillas In: Grow NB, Gursky-Doyen S, Krzton A, editors. High Altitude Primates. New York, NY: Springer New York. pp. 247–264. doi:10.1007/978-1-4614-8175-1_14

Roy J, Arandjelovic M, Bradley BJ, Guschanski K, Stephens CR, Bucknell D, Cirhuza H, Kusamba C, Kyungu JC, Smith V, Robbins MM, Vigilant L. 2014. Recent divergences and size decreases of eastern gorilla populations. *Biol Lett* **10**:20140811. doi:10.1098/rsbl.2014.0811

1407 Ruff CB, Junno J-A, Burgess ML, Canington SL, Harper C, Mudakikwa A, McFarlin SC.
1408 2022. Body proportions and environmental adaptation in gorillas. *American Journal of*
1409 *Biological Anthropology* **177**:501–529. doi:10.1002/ajpa.24443
1410 Salazar G. 2019. EcolUtils: Utilities for community ecology analysis. *R Package Version 0 1*
1411 *Available online: https://github com/GuillemSalazar/EcolUtils (accessed on 22 October*
1412 *2019)*.
1413 Salter SJ, Cox MJ, Turek EM, Calus ST, Cookson WO, Moffatt MF, Turner P, Parkhill J,
1414 Loman NJ, Walker AW. 2014. Reagent and laboratory contamination can critically
1415 impact sequence-based microbiome analyses. *BMC Biol* **12**:87. doi:10.1186/s12915-
1416 014-0087-z
1417 Sawafuji R, Saso A, Suda W, Hattori M, Ueda S. 2020. Ancient DNA analysis of food
1418 remains in human dental calculus from the Edo period, Japan. *PLoS One* **15**:e0226654.
1419 doi:10.1371/journal.pone.0226654
1420 Schmieder R, Edwards R. 2011. Quality control and preprocessing of metagenomic datasets.
1421 *Bioinformatics* **27**:863–864. doi:10.1093/bioinformatics/btr026
1422 Schubert M, Lindgreen S, Orlando L. 2016. AdapterRemoval v2: rapid adapter trimming,
1423 identification, and read merging. *BMC Res Notes* **9**:88. doi:10.1186/s13104-016-1900-2
1424 Segata N, Börnigen D, Morgan XC, Huttenhower C. 2013. PhyloPhlAn is a new method for
1425 improved phylogenetic and taxonomic placement of microbes. *Nat Commun* **4**:2304.
1426 doi:10.1038/ncomms3304
1427 Segata N, Waldron L, Ballarini A, Narasimhan V, Jousson O, Huttenhower C. 2012.
1428 Metagenomic microbial community profiling using unique clade-specific marker genes.
1429 *Nat Methods* **9**:811–814. doi:10.1038/nmeth.2066
1430 Shaiber A, Willis AD, Delmont TO, Roux S, Chen L-X, Schmid AC, Yousef M, Watson AR,
1431 Lolans K, Esen ÖC, Lee STM, Downey N, Morrison HG, Dewhirst FE, Mark Welch JL,
1432 Eren AM. 2020. Functional and genetic markers of niche partitioning among enigmatic
1433 members of the human oral microbiome. *Genome Biol* **21**:292. doi:10.1186/s13059-020-
1434 02195-w
1435 Shannon CE. 1948. A mathematical theory of communication. *The Bell System Technical*
1436 *Journal* **27**:379–423. doi:10.1002/j.1538-7305.1948.tb01338.x
1437 Shenhav L, Thompson M, Joseph TA, Briscoe L, Furman O, Bogumil D, Mizrahi I, Pe'er I,
1438 Halperin E. 2019. FEAST: fast expectation-maximization for microbial source tracking.
1439 *Nat Methods* **16**:627–632. doi:10.1038/s41592-019-0431-x
1440 Smith SN, Colston TJ, Siler CD. 2021. Venomous Snakes Reveal Ecological and
1441 Phylogenetic Factors Influencing Variation in Gut and Oral Microbiomes. *Front*
1442 *Microbiol* **12**:657754. doi:10.3389/fmicb.2021.657754
1443 Soares-Castro P, Araújo-Rodrigues H, Godoy-Vitorino F, Ferreira M, Covelo P, López A,
1444 Vingada J, Eira C, Santos PM. 2019. Microbiota fingerprints within the oral cavity of
1445 cetaceans as indicators for population biomonitoring. *Sci Rep* **9**:13679.
1446 doi:10.1038/s41598-019-50139-7
1447 Socransky SS, Haffajee AD, Cugini MA, Smith C, Kent RL. 1998. Microbial complexes in
1448 subgingival plaque. *Journal of Clinical Periodontology*. doi:10.1111/j.1600-
1449 051x.1998.tb02419.x
1450 Suzuki TA. 2017. Links between Natural Variation in the Microbiome and Host Fitness in
1451 Wild Mammals. *Integr Comp Biol* **57**:756–769. doi:10.1093/icb/icx104
1452 Takenoshita Y, Yamagiwa J. 2008. Estimating gorilla abundance by dung count in the
1453 northern part of Moukalaba-Doudou National Park, Gabon. *African Study Monographs*
1454 *Supplementary Issue* **39**:41–54.

Teles R, Wang C-Y. 2011. Mechanisms involved in the association between peridontal diseases and cardiovascular disease. *Oral Diseases*. doi:10.1111/j.1601-0825.2010.01784.x

Tonkin-Hill G, MacAlasdair N, Ruis C, Weimann A, Horesh G, Lees JA, Gladstone RA, Lo S, Beaudoin C, Floto RA, Frost SDW, Corander J, Bentley SD, Parkhill J. 2020. Producing polished prokaryotic pangenomes with the Panaroo pipeline. *Genome Biol* **21**:180. doi:10.1186/s13059-020-02090-4

Truong DT, Franzosa EA, Tickle TL, Scholz M, Weingart G, Pasolli E, Tett A, Huttenhower C, Segata N. 2015. MetaPhlAn2 for enhanced metagenomic taxonomic profiling. *Nat Methods* **12**:902–903. doi:10.1038/nmeth.3589

Tsuchida S, Kakooza S, Mbehang Nguema PP, Wampande EM, Ushida K. 2018. Characteristics of Gorilla-Specific Lactobacillus Isolated from Captive and Wild Gorillas. *Microorganisms* **6**. doi:10.3390/microorganisms6030086

Tsuchida S, Kitahara M, Nguema PPM, Norimitsu S, Fujita S, Yamagiwa J, Ngomanda A, Ohkuma M, Ushida K. 2014. Lactobacillus gorillae sp. nov., isolated from the faeces of captive and wild western lowland gorillas (Gorilla gorilla gorilla). *Int J Syst Evol Microbiol* **64**:4001–4006. doi:10.1099/ijs.0.068429-0

Tsuchida S, Nezuo M, Tsukahara M, Ogura Y, Hayashi T, Ushida K. 2015. Draft Genome Sequence of Lactobacillus gorillae Strain KZ01T, Isolated from a Western Lowland Gorilla. *Genome Announc* **3**. doi:10.1128/genomeA.01196-15

Tsuzukibashi O, Uchibori S, Kobayashi T, Umezawa K, Mashimo C, Nambu T, Saito M, Hashizume-Takizawa T, Ochiai T. 2017. Isolation and identification methods of Rothia species in oral cavities. *J Microbiol Methods* **134**:21–26. doi:10.1016/j.mimet.2017.01.005

Turner LA, Bucking C. 2019. The role of intestinal bacteria in the ammonia detoxification ability of teleost fish. *J Exp Biol* **222**. doi:10.1242/jeb.209882

Uritskiy GV, DiRuggiero J, Taylor J. 2018. MetaWRAP—a flexible pipeline for genome-resolved metagenomic data analysis. *Microbiome* **6**:158. doi:10.1186/s40168-018-0541-1

van der Hoek Y, Pazo WD, Binyinyi E, Ngobobo U, Stoinski TS, Caillaud D. 2021. Diet of Grauer's Gorillas (Gorilla beringei graueri) in a Low-Elevation Forest. *Folia Primatol* **92**:126–138. doi:10.1159/000515377

van der Valk T, Díez-Del-Molino D, Marques-Bonet T, Guschanski K, Dalén L. 2019. Historical Genomes Reveal the Genomic Consequences of Recent Population Decline in Eastern Gorillas. *Curr Biol* **29**:165–170.e6. doi:10.1016/j.cub.2018.11.055

van der Valk T, Lona Durazo F, Dalén L, Guschanski K. 2017. Whole mitochondrial genome capture from faecal samples and museum-preserved specimens. *Mol Ecol Resour* **17**:e111–e121. doi:10.1111/1755-0998.12699

van der Valk T, Sandoval-Castellanos E, Caillaud D, Ngobobo U, Binyinyi E, Nishuli R, Stoinski T, Gilissen E, Sonet G, Semal P, Kalthoff DC, Dalén L, Guschanski K. 2018. Significant loss of mitochondrial diversity within the last century due to extinction of peripheral populations in eastern gorillas. *Sci Rep* **8**:6551. doi:10.1038/s41598-018-24497-7

van der Valk T, Vezzi F, Ormestad M, Dalén L, Guschanski K. 2020. Index hopping on the Illumina HiseqX platform and its consequences for ancient DNA studies. *Mol Ecol Resour* **20**:1171–1181. doi:10.1111/1755-0998.13009

Velsko IM, Fellows Yates JA, Aron F, Hagan RW, Frantz LAF, Loe L, Martinez JBR, Chaves E, Gosden C, Larson G, Warinner C. 2019. Microbial differences between

1503 dental plaque and historic dental calculus are related to oral biofilm maturation stage.
1504 *Microbiome* **7**:102. doi:10.1186/s40168-019-0717-3
1505 Velsko IM, Frantz LAF, Herbig A, Larson G, Warinner C. 2018. Selection of Appropriate
1506 Metagenome Taxonomic Classifiers for Ancient Microbiome Research. *mSystems* **3**.
1507 doi:10.1128/mSystems.00080-18
1508 Vuong HE, Yano JM, Fung TC, Hsiao EY. 2017. The Microbiome and Host Behavior. *Annu*
1509 *Rev Neurosci* **40**:21–49. doi:10.1146/annurev-neuro-072116-031347
1510 Wade WG. 2013. The oral microbiome in health and disease. *Pharmacol Res* **69**:137–143.
1511 doi:10.1016/j.phrs.2012.11.006
1512 Warinner C. 2016. Dental Calculus and the Evolution of the Human Oral Microbiome. *J*
1513 *Calif Dent Assoc* **44**:411–420.
1514 Warinner C, Rodrigues JFM, Vyas R, Trachsel C, Shved N, Grossmann J, Radini A, Hancock
1515 Y, Tito RY, Fiddyment S, Speller C, Hendy J, Charlton S, Luder HU, Salazar-García
1516 DC, Eppler E, Seiler R, Hansen LH, Castruita JAS, Barkow-Oesterreicher S, Teoh KY,
1517 Kelstrup CD, Olsen JV, Nanni P, Kawai T, Willerslev E, von Mering C, Lewis CM Jr,
1518 Collins MJ, Gilbert MTP, Rühli F, Cappellini E. 2014. Pathogens and host immunity in
1519 the ancient human oral cavity. *Nat Genet* **46**:336–344. doi:10.1038/ng.2906
1520 Warinner C, Speller C, Collins MJ. 2015. A new era in palaeomicrobiology: prospects for
1521 ancient dental calculus as a long-term record of the human oral microbiome. *Philos*
1522 *Trans R Soc Lond B Biol Sci* **370**:20130376. doi:10.1098/rstb.2013.0376
1523 West CE, Rydén P, Lundin D, Engstrand L, Tulic MK, Prescott SL. 2015. Gut microbiome
1524 and innate immune response patterns in IgE-associated eczema. *Clin Exp Allergy*
1525 **45**:1419–1429. doi:10.1111/cea.12566
1526 Weyrich LS, Farrer AG, Eisenhofer R, Arriola LA, Young J, Selway CA, Handsley-Davis M,
1527 Adler CJ, Breen J, Cooper A. 2019. Laboratory contamination over time during low-
1528 biomass sample analysis. *Molecular Ecology Resources*. doi:10.1111/1755-0998.13011
1529 Wheeler QD. 2004. What if GBIF? *Bioscience* **54**:718. doi:10.1641/0006-
1530 3568(2004)054[0718:wig]2.0.co;2
1531 Williamson EA, Maisel FG, Groves CP, Fruth BI, Humle T, Morton FB, Richardson MC,
1532 Russon AE, Singleton I. 2013. Family Hominidae (Great Apes) In: Mittermeier RA,
1533 Rylands AB, Wilson DE, editors. Handbook of the Mammals of the World: Primates.
1534 Lynx Edicions in association with Conservation International and IUCN.
1535 Wood DE, Lu J, Langmead B. 2019. Improved metagenomic analysis with Kraken 2.
1536 *Genome Biol* **20**:257. doi:10.1186/s13059-019-1891-0
1537 Wu Y-W, Simmons BA, Singer SW. 2016. MaxBin 2.0: an automated binning algorithm to
1538 recover genomes from multiple metagenomic datasets. *Bioinformatics* **32**:605–607.
1539 doi:10.1093/bioinformatics/btv638
1540 Xue Y, Prado-Martinez J, Sudmant PH, Narasimhan V, Ayub Q, Szpak M, Frandsen P, Chen
1541 Y, Yngvadottir B, Cooper DN, de Manuel M, Hernandez-Rodriguez J, Lobon I,
1542 Siegismund HR, Pagani L, Quail MA, Hvilsom C, Mudakikwa A, Eichler EE, Cranfield
1543 MR, Marques-Bonet T, Tyler-Smith C, Scally A. 2015. Mountain gorilla genomes
1544 reveal the impact of long-term population decline and inbreeding. *Science* **348**:242–245.
1545 doi:10.1126/science.aaa3952
1546 Xu X, Arnason U. 1996. A complete sequence of the mitochondrial genome of the western
1547 lowland gorilla. *Mol Biol Evol* **13**:691–698.
1548 doi:10.1093/oxfordjournals.molbev.a025630
1549 Yamagiwa J, Basabose AK, Kaleme KP, Yumoto T. 2008. Phenology of fruits consumed by
1550 a sympatric population of gorillas and chimpanzees in Kahuzibiega National Park,

Democratic Republic of Congo. *African Study Monographs Supplementary Issue* **39**:3–22.

Yamagiwa J, Basabose AK, Kaleme K, Yumoto T. 2005. Diet of grauer's gorillas in the Montane forest of kahuzi, democratic republic of Congo. *Int J Primatol* **26**:1345–1373. doi:10.1007/s10764-005-8856-8

Yan J, Li Y, Han XZ, Chen WF, Zou WX, Xie Z, Li M. 2017. Agrobacterium deltaense sp. nov., an endophytic bacteria isolated from nodule of Sesbania cannabina. *Arch Microbiol* **199**:1003–1009. doi:10.1007/s00203-017-1367-0

Youngblut ND, de la Cuesta-Zuluaga J, Reischer GH, Dauser S, Schuster N, Walzer C, Stalder G, Farnleitner AH, Ley RE. 2020. Large-Scale Metagenome Assembly Reveals Novel Animal-Associated Microbial Genomes, Biosynthetic Gene Clusters, and Other Genetic Diversity. *mSystems* **5**. doi:10.1128/mSystems.01045-20

Youngblut ND, Reischer GH, Walters W, Schuster N, Walzer C, Stalder G, Ley RE, Farnleitner AH. 2019. Host diet and evolutionary history explain different aspects of gut microbiome diversity among vertebrate clades. *Nat Commun* **10**:2200. doi:10.1038/s41467-019-10191-3

Yu G, Smith DK, Zhu H, Guan Y, Lam TT-Y. 2017. Ggtree : An r package for visualization and annotation of phylogenetic trees with their covariates and other associated data. *Methods Ecol Evol* **8**:28–36. doi:10.1111/2041-210x.12628